IFT - UNESP
INSTITUTO DE FÍSICA TEÓRICA

DISSERTAÇÃO DE MESTRADO IFT-D.16/2022

ABSORBTION STATISTICS OF MOVEMENT MODELS WITH HOME-RANGING BEHAVIOR

Benjamin Garcia de Figueiredo

Orientador

Ricardo Martínez-García

DEZEMBRO 2022

Figueiredo, Benjamin Garcia de
F475a Absorbtion statistics of movement models with home-ranging behavior / Benjamin Garcia de Figueiredo. – São Paulo, 2022
97 f.

Dissertação (mestrado) – Universidade Estadual Paulista (Unesp), Instituto de Física Teórica (IFT), São Paulo
Orientador: Ricardo Martínez-García

1. Ecologia. 2. Processo estocástico. 3. Biofísica. I. Título

Sistema de geração automática de fichas catalográficas da Unesp. Biblioteca do Instituto de Física Teórica (IFT), São Paulo. Dados fornecidos pelo autor(a).

In memory of my father

Acknowledgements

I am first and foremost very grateful for the support of my advisor Ricardo Martínez-García throughout and beyond this project. Ricardo has advocated for me and my work from the first day of our collaboration, and I owe much of my personal and professional growth to his kindness and encouragement these past three years. This gratitude has to be extended to the wonderful group Ricardo assembled. My work benefited from many fruitful discussions with the post-docs at our group, Drs. Gabriel Andreguetto Maciel, Jesus Mauricio Ancinas, Pablo de Castro, Vivian Dornelas, and my fellow graduate colleagues Daniel Cardoso, Jairo Rojas, João Valeriano and Rafael Mena.

Our work was made possible by the generous funding from: FAPESP, through my Master's fellowship, process number 2019/26736-0, associated to Ricardo's Young Researcher Grant, process number 2019/05523-8; Instituto Serrapilheira for their grant, which allowed me to extend my Master's fellowship, as well as their fellowship throughout the 2022 Training Program in Quantitative Biology and Ecology, jointly organized with ICTP-SAIFR.

Major thanks go out to the teams at IFT-Unesp and ICTP-SAIFR for creating such a rich academic environment with so many opportunities. In particular I would like to thank Jandira Ferreira Oliveira, Luzinete Aparecida Martins and Professors Nathan Jacob Berkovits and Gastão Krein for their tremendous help at various critical junctures in this process.

The development of my work and the writing of this dissertation would have been much less enjoyable were it not for the presence of my various friends at IFT and from the QBio Training Program, to whom I owe many moments of joy throughout these years. I have to furthermore thank professors Roland Köberle and William Bialek for lighting in me the passion for biological physics at the end of my undergraduate studies.

Finally, I have to thank my family, in particular my mother Claudilene, my late father Haroldo and my brother Joaquim for nurturing my love of science from a very early age and for their unconditional support of my pursuits throughout the years for as long as I can remember.

Resumo

Populações ecológicas usam, em geral, o espaço ao seu redor de uma forma inomogênea, e essa não-homogeneidade modula suas interações locais. Apesar da existência de áreas de vida sabidamenta afetar observáveis importantes como taxas de encontros entre indivíduos, muitos modelos em dinâmica de populações explicita- ou implicitamente assumem que populações fazem uso homogêneo do space.

O processo de Ornstein-Uhlenbeck (OU) é um processo estocástico espacial que possui as características básicas de movimento limitado a uma área de vida. Neste *framework* the modelos de movimento OU, as estatisticas de encontro entre processos simultâneos servem como um indicador da estatística de interações entre indivíduos, enquanto estatísticas de encontro de um processo com um domínio espacial servem como um indicador da estatística de interações entre um indivíduo e características do seu ambiente como pistas ou cercas. Apesar de problemas matemáticos parecido já terem sido investigados, especialmente em uma dimensão, menos estudos abordam a situação mais ecologicamente relevante de duas dimensões (2D), ou cenários com interações probabilísticas.

No presente trabalho, desenvolvemos um ferramentário geral para o estudo de interações probabilísticas em processos estocásticos, e conduzimos um estudo analítico de dois problemas desse tipo. Primeiramente, estudamos as estatísticas de interações the um modelo OU 2D isotrópico com uma pista. Investigamos, então, as estatísticas de encontro de dois modelos OU idênticos e isotrópicos em 2D.

Nossos resultados podem ajudar na construção de fundações mais mecanísticas e realistas de modelos de dinâmica de populações e de decisões de conservação, baseados em escalonar interações de indivíduoas à escala de processos ecológicos ou evolutivos.

Palavras Chaves: Ecologia; Movimento; Processos Estocásticos;

Áreas do conhecimento: Física; Física Estatística; Física Biológica.

Abstract

Ecological populations are, in general, not well mixed, and their non-homogeneous use of space modulates their local interactions. Although this range-residency is known to affect important observables such as encounter rates between individuals, many models in population dynamics implicitly or explicitly assume that populations make homogenous use of space.

The Ornstein-Uhlenbeck (OU) process is a stochastic process in space that displays the basic characteristics of movement bounded by and centered around a home-range. Within the framework of OU movement models, the crossing statistics of simultaneous processes serve as a proxy for the interaction statistics between individuals, while the encounter statistics of a process with a domain serve as a proxy for the interaction statistics of an individual with features of the environment such as roads or fences. While similar mathematical problems have been investigated, especially in one dimension, fewer studies have addressed the more ecologically relevant two-dimensional case (2D), or of situations with imperfect absorption, which could represent scenarios with probabilistic interactions.

In this work, we develop a general framework for probabilistic interactions in stochastic processes, and conduct an analytical study of two problems of this kind. Firstly the interaction statistics of an isotropic 2D OU particle with a "road". We explore the connection between the continuous model given by partial differential equations and its discretization, which more closely resembles observation.

We then investigate the first-crossing statistics of two identical isotropic OU particles in 2D. More generally, we see how to treat encounters between multiple individuals.

Our results could help build the foundations of more mechanistic and realistic models of optimal search, population dynamics and conservation decision-making, based on the scaling up of individual interactions to the scale of ecological or evolutionary processes.

Keywords: Ecology; Movement; Stochastic Processes;

Knowledge areas: Physics; Statistical Physics; Biophysics.

Contents

Chapter 1

Introduction

Many of the major challenges in modern biology involve representing theoretically the mechanisms underlying the behavior of living systems so as to integrate phenomena at different scales. In the context of ecology, one such challenge involves connecting individual movement-level processes to population-scale consequences.

Much of the work in the fields of population dynamics and conservation decision-making involves phenomenological or effective descriptions of the systems involved. As with any model, their explanatory ability is always limited by which concepts — e.g. population — are treated as irreducible. Biology always involves phenomena at various scales, both larger and smaller than the "focal" scale of a model. This is where having more mechanistic descriptions of these basic ecological processes becomes very important. Take, for example, the ecoevolutionary dynamics of a population where sexual selection is based on movement-behavior. In this situation, a description of the mesoscale — population — will require an understanding of the interplay between the macroscale — selection — and the microscale — movement strategies.

In the era of large movement datasets [1, 2], with increasingly precise and sophisticated techniques employed [3, 4] increased interest in conservation ecology and eco-evolutionary processes, we find ourselves still lacking a principled understanding of how interactions should be understood in the context of movement, which is a central way animals interact with their surroundings.

The present work aims to develop techniques and unfold some ideas towards this general goal. We utilize movement models to represent local spatial interactions. In Chapter 2, we briefly review the basic formalism utilized to study stochastic dynamical systems. Then, in Chapter 3, we develop a framework for interactions between an animal and a fixed domain in their environment, and analytically solve the particular case of a road in a two-dimensional landscape. In Chapter 4, we show how interactions between individuals can be incorporated in the previous framework, and analytically solve the simplest such scenario,

involving two identical individuals. Finally, in Chapter 5, we discuss the merits of the project and next steps.

Chapter 2

Animal movement and random motion

The often tortuous landscape-scale movement patterns of animals reflect a combination of the various environmental irregularities, navigational restrictions and perceptual capabilities which, taken together, create complex, layered patterns [5]. Some of these factors shape the large scale and long term properties of motion. Others operate at a smaller scale where their highly contingent nature makes them only amenable to a statistical description — in other words, they operate as noise.

There are many relevant characteristics of movement one may take into account when creating a model. One that has wide-reaching implications is **range-residency** [6, 7], that is, the tendency of an animal to live in a localized region of their environment. Since this implies a highly inhomogeneous use of space, it can be a point of failure of various models which traditionally employ mean-field approaches. These ultimately assume the law of mass action for interactions between populations, which tends to only hold if space is occupied uniformely [7].

The interplay between directed, ballistic motion and random, diffusive motion is the object of study of **stochastic dynamics** [8, 9]. In this chapter, we briefly review the theory of stochastic differential equations with white noise and their various descriptions — from microscopic to macroscopic. We then elaborate on the particular case of the Ornstein-Uhlenbeck process [10], which will serve as the object of theoretical study throughout the following chapters.

2.1 Stochastic calculus

The entire intuition behind (Gaussian) stochastic dynamics is the Langevin equation for Brownian motion [11, 12], which deals with a continuous process $W(t)$ which responds to a time-dependent Gaussian white noise $\xi(t)$, described as

$$\frac{\mathrm{d}W}{\mathrm{d}t} = \xi(t) \tag{2.1}$$

$$W(0) = 0 \tag{2.2}$$

$$\langle \xi(t) \rangle = 0 \tag{2.3}$$

$$\langle \xi(t)\xi(t') \rangle = \delta(t - t'), \tag{2.4}$$

where $\langle \cdot \rangle \equiv \mathbb{E}[\cdot]$ represents averaging over realizations. Since we can explicitly integrate the equation above, we find

$$W(t) = \int_0^t \xi(t')\mathrm{d}t', \tag{2.5}$$

which, in particular, gives, for $s < t$,

$$\langle W(t) \rangle = 0, \tag{2.6}$$

$$\langle W(t)W(t) \rangle = \int_0^t \int_0^t \langle \xi(t')\xi(t'') \rangle \mathrm{d}t'\mathrm{d}t'' = t. \tag{2.7}$$

We have defined $\xi(t)$ to be a Gaussian process, so all higher moments of the distribution can be derived from the first and second moments — the so-called Wick theorem. This also means $W(t) \sim \mathcal{N}(0, t)$, where $\mathcal{N}(\boldsymbol{\mu}, \Sigma)$ denotes a (possibly multivariate) normal distribution with mean $\boldsymbol{\mu}$ and covariance matrix Σ. This is what fully characterizes the solution $W(t)$, which is called the (one-dimensional) **Wiener process**. In higher dimensions, we write $\boldsymbol{W}(t)$ for a vector of independent realizations of the one-dimensional process.

Consider now the process $\boldsymbol{x}(t)$ which may represent the spatial trajectory of an animal as observed using an idealized tracking device. Since $\boldsymbol{W}(t)$ is almost-surely non-differentiable, it is conventional for a stochastic differential equation for the process $\boldsymbol{x}(t)$ to be written in the form

$$\mathrm{d}\boldsymbol{x} = \boldsymbol{\mu}(\boldsymbol{x}(t), t)\mathrm{d}t + \sqrt{g(\boldsymbol{x}(t), t)}\mathrm{d}\boldsymbol{W}(t), \tag{2.8}$$

$$\boldsymbol{x}(0) = \boldsymbol{x}_0, \tag{2.9}$$

which should be seen as a kind of short-hand for the integral equation

$$\boldsymbol{x}(t) - \boldsymbol{x}_0 = \int_0^t \left(\boldsymbol{\mu}(\boldsymbol{x}(t'), t') + \sqrt{g(\boldsymbol{x}(t'), t')}\boldsymbol{\xi}(t') \right) \mathrm{d}t', \tag{2.10}$$

with the first term is a deterministic drift and the second is stochastic.

2.1.1 Ornstein-Uhlenbeck process

The process in particular we take to represent a range-residing animal is the (isotropic) **Ornstein-Uhlenbeck (OU) process**, namely

$$\mathrm{d}\boldsymbol{x} = \frac{(\boldsymbol{\lambda} - \boldsymbol{x})}{\tau}\mathrm{d}t + \sqrt{g}\mathrm{d}\boldsymbol{W}(t). \tag{2.11}$$

Here, the parameter $\boldsymbol{\lambda}$ is a center of attraction, to which the system relaxes with a characteristic time scale τ. Noise is modulated in amplitude by the parameter g.

The Ornstein-Uhlenbeck process has a long story of success in describing home-ranging animals, from describing trajectories from radio telemetry data [13] to modern analyses of distributions of encounters using GPS tracking [14]. It provides, furthermore, a powerful theoretical basis for analyses of these same objects [6, 7].

The solution of the isotropic OU process may be derived quite straightforwardly, noting that

$$\mathrm{d}\left(\exp(t/\tau)\boldsymbol{x}\right) = \exp(t/\tau)\left(\frac{\boldsymbol{\lambda}}{\tau}\mathrm{d}t + \sqrt{g}\mathrm{d}\boldsymbol{W}(t)\right) \tag{2.12}$$

we can immediately write

$$\begin{aligned}\boldsymbol{x}(t) &= \boldsymbol{x}_0\exp(-t/\tau) + \exp(-t/\tau)\int_0^t \exp\left(t'/\tau\right)\left(\frac{\boldsymbol{\lambda}}{\tau}\mathrm{d}t' + \sqrt{g}\mathrm{d}\boldsymbol{W}(t')\right)\\ &= x_0\exp(-t/\tau) + (1-\exp(-t/\tau))\boldsymbol{\lambda}\\ &+ \sqrt{g}\exp(-t/\tau)\int_0^t \exp\left(t'/\tau\right)\mathrm{d}\boldsymbol{W}(t').\end{aligned} \tag{2.13}$$

Ultimately

$$\langle\boldsymbol{x}(t)\rangle = x_0\exp(-t/\tau) + (1-\exp(-t/\tau))\boldsymbol{\lambda}, \tag{2.14}$$

$$\langle(\boldsymbol{x}(t) - \langle x(t)\rangle)^2\rangle = \frac{g\tau}{2}\left(1-\exp(-2t/\tau)\right). \tag{2.15}$$

The previous results means that, asymptotically, the trajectory converges to a stationary process with $\boldsymbol{x} \sim \mathcal{N}\left(\boldsymbol{\lambda}, \mathrm{diag}\left(\frac{g\tau}{2}\right)\right)$. This stationary distribution is what characterizes the home-range, which is this region of space of characteristic length-scale $\sqrt{g\tau}$.

2.2 Kolmogorov and Fokker-Planck equations

In the following we consider a general SDE of the form

$$\mathrm{d}\boldsymbol{x}(t) = \boldsymbol{\mu}(\boldsymbol{x}(t), t)\mathrm{d}t + \sqrt{g(\boldsymbol{x}(t), t)}\mathrm{d}\boldsymbol{W}(t) \tag{2.16}$$

with $\mathrm{d}W$ standard Brownian motion. When taking the differential of any function of x, we must remember one of the defining properties of W, namely that its increments are independent, normally distributed variables with variance proportional to time. Applying this to $\mathrm{d}W$, we see that formally

$$\mathrm{d}\boldsymbol{W}(t) = \sqrt{\mathrm{d}t}\boldsymbol{Z} \tag{2.17}$$

for some standard normal distributed variable $\boldsymbol{Z}$, that is, where each component $Z_i \sim \mathcal{N}(0, 1)$. Thus, for each component i, $\mathrm{d}W_i^2/\mathrm{d}t$ is a chi-square variable with one degree of freedom, so $\langle \mathrm{d}W_i^2 \rangle = \mathrm{d}t$. This mean that, taking some arbitrary observable $f(\boldsymbol{x}, t)$, its differential can be written

$$\mathrm{d}f = \frac{\partial f}{\partial t}\mathrm{d}t + \frac{\partial f}{\partial \boldsymbol{x}} \cdot \mathrm{d}\boldsymbol{x} + \frac{1}{2}\sum_{ij} \frac{\partial^2 f}{\partial x_i \partial x_j}\mathrm{d}x_i \mathrm{d}x_j + \cdots \tag{2.18}$$

We specialize to the case of a one-dimensional process $x(t)$, since the higher-dimensional generalization is quite straightforward. Along the solutions of (2.8), one can rewrite, substituting $\mathrm{d}x(t)$ and staying to linear order in $\mathrm{d}t$ and quadratic in $\mathrm{d}W$:

$$\mathrm{d}f = \left[\frac{\partial f}{\partial t} + \mu(x, t)\frac{\partial f}{\partial x}\right]\mathrm{d}t + \sqrt{g(x, t)}\frac{\partial f}{\partial x}\mathrm{d}W(t) + + \frac{g(x, t)}{2}\frac{\partial^2 f}{\partial x^2}\mathrm{d}W(t)^2. \tag{2.19}$$

We can now integrate (2.19) over some finite time interval $[s, t]$ and take the expected value conditioned on the initial value $x(s) = x_s$ to find, using the fact W is zero-mean,

$$\begin{aligned}
&\mathbb{E}[f(x(t))|x(s)=x_s] - f(x_s) = \\
&\qquad = \left\langle \int_s^t \left[\frac{\partial}{\partial t'} + \mu(x,t')\frac{\partial}{\partial x} + \frac{g(x,t')}{2}\frac{\partial^2}{\partial x^2} \right] f(x(t'),t')\mathrm{d}t' \right\rangle \\
&\qquad = \left\langle \int_s^t \left(L_x^\dagger(t') + \frac{\partial}{\partial t'} \right) f(x(t'),t')\mathrm{d}t' \right\rangle_{x(s)=x_s}, \\
&\text{where } L_x^\dagger(t') \equiv \mu(x,t')\frac{\partial}{\partial x} + \frac{g(x,t')}{2}\frac{\partial^2}{\partial x^2},
\end{aligned} \tag{2.20}$$

with the operator $L_x^\dagger$ — here defined as an adjoint purely as a matter of convention — the so-called **generator of diffusion**. This allows in particular for us to obtain a differential equation for the backward time-evolution of the system — that is, with final conditions held fixed [12]. We can construct, for any time-independent observable $f(x)$, an associated time-dependent $u(x_s,s) \equiv \mathbb{E}[f(x(t))|x(s)=x_s]$. It holds, in particular, from (2.20), that

$$\begin{aligned}
&\lim_{t\to s} \frac{\langle u(x(t),t)\rangle_{x(s)=x_s} - f(x_s)}{s-t} = \\
&\qquad = \lim_{t\to s} \frac{1}{s-t} \left\langle \int_s^t \left(L^\dagger + \frac{\partial}{\partial t'} \right) u(x(t'),t')\mathrm{d}t' \right\rangle_{x(s)=x_s} \\
&\qquad = \left(L_{x_s}^\dagger + \frac{\partial}{\partial s} \right) u(x_s,s)
\end{aligned} \tag{2.21}$$

where the mean value theorem makes it so that only the integrand evaluated at $t' = s$ remains. Now, a particular consequence of the definition of u is that $u(x(t),t) = f(x(t))$. But then, on the LHS, we can identify $\langle u(x(t),t)\rangle_{x(s)=x_s}$ with $u(x_s,s)$ itself for all t, making the entire numerator term identically zero. What results is the so-called **Kolmogorov backward equation** for the backward time evolution (after all, x_s is by construction an initial condition) of the expected value of the observable f,

$$\left(\frac{\partial}{\partial s} + L_{x_s}^\dagger \right) \mathbb{E}\left[f(x(t))|x(s)=x_s\right] = 0 \qquad s < t \tag{2.22}$$

$$\mathbb{E}\left[f(x(t))|x(t)=x_s\right] = f(x_s) \tag{2.23}$$

An important consequence of (2.22) can be seen when the expectation value

of f is explicitly written in terms of the transition probability $P(x,t|x_s,s)\mathrm{d}x \equiv \mathbb{P}\left[x < x(t) < x + \mathrm{d}x | x(s) = x_s\right]$. Indeed, since by definition we have

$$\mathbb{E}\left[f(x(t))|x(s) = x_s\right] = \int f(x)P(x,t|x_s,s)\mathrm{d}x, \tag{2.24}$$

we immediately conclude that

$$\int f(x)\left(\frac{\partial}{\partial s} + L^\dagger_{x_s}\right)P(x,t|x_s,s)\mathrm{d}x = 0 \tag{2.25}$$

and notice this holds for any observable f whatsoever to conclude that the transition probability too solves the Kolmogorov backward equation.

This result is useful in particular when the process is time homogeneous. There we can write $P(x,t|x_s,s) = P(x,t-s|x_0,0)$, or more simply $P(x,t-s|x_0)$. A change of variables $t - s \mapsto t$, so $\partial_s \to -\partial_t$, gives us what we call the **backwards Fokker-Planck equation**

$$\left(\frac{\partial}{\partial t} - L^\dagger_{x_0}\right)P(x,t|x_0) = 0, \qquad t > 0, \tag{2.26}$$

$$P(x,0|x_0) = \delta(x - x_0). \tag{2.27}$$

One way to understand the backwards Fokker-Planck equation is as a kind of distribution-level dynamics of the system, which nevertheless starts at one well-defined position in space. As such, we may consider it as a "mesoscopic" description of the system, where the output is the statistics of all possible forward evolutions from a starting point.

2.2.1 The forward equation

A final consequence of the backwards Fokker-Planck equation is attained by considering the following identity, which follows simply from the definition of $L^\dagger$,

$$\int f(x)P(x,t|x_0)\mathrm{d}x - f(x_0) = \int_0^t \int (L^\dagger f)(x)P(x,t'|x_0)\mathrm{d}x\mathrm{d}t'. \tag{2.28}$$

Taking a time derivative on either side, we arrive at

$$\int f(x)\frac{\partial}{\partial t}P(x,t|x_0)\mathrm{d}x = \int (L^\dagger f)(x)P(x,t|x_0)\mathrm{d}x, \tag{2.29}$$

or, by definition of the adjoint,

$$\int f(x)\frac{\partial}{\partial t}P(x,t|x_0)\mathrm{d}x = \int f(x)L_x P(x,t|x_0)\mathrm{d}x. \tag{2.30}$$

Again, since f is arbitrary, we can state that the following equation holds

$$\frac{\partial}{\partial t}P(x,t|x_0) = L_x P(x,t|x_0), \tag{2.31}$$

$$P(x,0|x_0) = \delta(x-x_0). \tag{2.32}$$

In particular, if we have some distribution of initial conditions $P_0(x_0)$, we can find an equation for the future distribution $P(x,t)$ given by multiplying the above equations by $P_0(x_0)$ and propagating forward in time, to find

$$\frac{\partial}{\partial t}P(x,t) = LP(x,t), \tag{2.33}$$

$$P(x,0) = P_0(x). \tag{2.34}$$

This is the **Fokker-Planck equation** for the system. It provides a truly "macroscopic" view of the time evolution of the system, dealing only with probability distributions. The operator L is accordingly denominated the **Fokker-Plank operator**.

2.2.2 First-passage statistics

A very important kind of problem which is deeply related to the questions which will be investigated in the next chapters is the so-called **first-passage problem**, which attempts to determine, for some region in the state-space $\Omega \subset \mathbb{R}^n$, the probability distribution of the quantity T defined as

$$T = \inf\{t \in [0,\infty) | x(t) \in \Omega\}. \tag{2.35}$$

Though there is a variety of approaches in first-passage theory, one of the simplest ways to understand this kind of problem is by looking at an absorbing process defined as

$$\text{(i) } \mathrm{d}\boldsymbol{x} = -\frac{\boldsymbol{x}}{\tau}\mathrm{d}t + \sqrt{g}\mathrm{d}\boldsymbol{W}_t \tag{2.36}$$

$$\text{(ii) Whenever } \boldsymbol{x}(t) \in \Omega, \text{ end the process.} \tag{2.37}$$

Which would correspond, macroscopically, to imposing Dirichlet boundary conditions on the Fokker-Planck equation describing the process $x(t)$, that is

$$\begin{aligned} \left(\frac{\partial}{\partial t} - L\right) P(x,t) &= 0, \\ P(x,0) &= P_0(x), \\ P(x,t)|_\Omega &= 0. \end{aligned} \tag{2.38}$$

This allows for a direct connection with the first-passage probability distribution via the **survival function** $S(t|x_0)$ defined as

$$S(t|x_0) \equiv \mathbb{P}[T > t | x(0) = x_0] = \int P(x,t|x_0)\mathrm{d}x. \tag{2.39}$$

Since the probability of "absorption" is $(1 - S(t|x_0))$, we can immediately find the probability density function of the first-passage time distribution by differentiation

$$\phi_\Omega(t|x_0) = \frac{\mathrm{d}}{\mathrm{d}t}(1 - S(t|x_0)) = -\frac{\mathrm{d}}{\mathrm{d}t}S(t|x_0). \tag{2.40}$$

This is where the backwards Fokker-Planck equation becomes very useful. Since $P(x,t|x_0)$ simultaneously solves the (forward) Fokker-Planck equation and its backwards counterpart simultaneously, we can integrate over x in (2.26) to immediately find that the survival function too solves the backwards Fokker-Planck equation. The initial condition is the immediate $S(0) = 1$. Furthermore, if we assume **recurrence** with respect to the boundary Ω, that is, that $x(t)$ will come across Ω almost-surely, we can say with certainty that $S(+\infty|x_0) = 0$, meaning

$$\begin{aligned} &\int_0^\infty \frac{\partial S(t|x_0)}{\partial t}\mathrm{d}t = L^\dagger_{x_0}\int_0^\infty S(t|x_0)\mathrm{d}t \\ \iff\ & S(+\infty) - S(0) = L^\dagger_{x_0}\left[tS(t|x_0)|_0^\infty - \int_0^\infty t\frac{\mathrm{d}}{\mathrm{d}t}S(t|x_0)\mathrm{d}t\right] \\ \iff\ & L^\dagger_{x_0}\int_0^\infty t\phi_\Omega(t|x_0) = L^\dagger_{x_0}\langle t\rangle_\Omega(x_0) = -1. \end{aligned} \tag{2.41}$$

This gives us, therefore, a differential equation for the mean first-passage time at Ω.

With these preliminary steps completed, we are now able to develop some theoretical frameworks for spatial interactions in home-ranging animals, which shall be done in the following chapters.

Chapter 3

Interactions of a home-ranging species with a road

One of the major ways by which human development alters the conditions of habitats worldwide is by modifying the spatial features of the environment. The rapid, drastic changes in land cover due to socio-economic growth over the past few centuries affect the lives of land animals on all scales, from imposing local constraints on behavior to disrupting migration patterns and gene flow [15]. Conversely, changes in the composition and distribution of biodiversity can have drastic adverse effects on human affairs. Human-wildlife conflicts often arising out of the alteration of a population's habitat include crop raiding, livestock depredation, zoonotic spillover but also more direct interactions leading to human injury and death [16].

Focusing on local spatiotemporal effects of an altered landscape, we come to the question of how animals interact with fixed built-up features introduced into their habitats. This includes roads, fences and buildings. A first proxy for quantifying interactions with a stationary object is the probability distribution of encounters with it purely due to motion. Of course, in general the pattern of movement of an organism may change in response to modifications of the surrounding environment, depending on its perceptual capabilities, as well as capacity for adaptation and learning [17]. The extent to which individuals are able to adapt to abrupt changes in their environment varies by taxa, and is in large part unknown. A better understanding of the patterns of motion arising in reaction to alterations in a landscape is an important step towards developing better strategies for intervention in conservation efforts.

In this chapter, we develop a theory for the interactions of a home-ranging land animal and a linear object in its environment. We assume tacitly that the individual's pattern of motion is unaffected by the presence of this object. An example of a system of interest this may model is that of wildlife-vehicle collisions

with giant anteaters (*Myrmecophaga tridactyla*), though there might be others such as powerline electrocutions in birds [18]. It has been assessed that the movement behavior of the giant anteater is mostly unchanged by the presence of roads, which end up becoming an important source of mortality for the species. Coupled with the fact that anteaters are unlikely to search for passage structures in their environment [19], it becomes important to systematically evaluate different strategies one might employ when it comes to road construction near their habitats.

3.1 Partially absorbing domains

To begin taking into account occupation-dependent probabilistic interactions in certain regions within the space used by an individual, we delimit some subset $\Omega \subseteq \mathbb{R}^2$ representing the locations of spatial features we are modelling. The possibility of an interaction between a realization of this process and this domain is represented by the inclusion of an absorbing state to the process, in such a way that the total spatial occupation probability $P(\boldsymbol{x}, t)$ will tend to in fact decrease in time. To each $\boldsymbol{x} \in \Omega$, we attribute a probability per unit time $\omega(\boldsymbol{x}, t)$ of absorption. Taking at this stage a home-range center $\boldsymbol{\lambda} = \mathbf{0}$ without loss of generality, this system is described by the "leaky" Fokker-Planck equation

$$\frac{\partial P(\boldsymbol{x}, t)}{\partial t} = \frac{1}{\tau} \boldsymbol{\nabla} \cdot (P(\boldsymbol{x}, t)\boldsymbol{x}) + \frac{g}{2} \boldsymbol{\nabla}^2 P(\boldsymbol{x}, t) - \omega(\boldsymbol{x}, t) P(\boldsymbol{x}, t). \tag{3.1}$$

Defining the probability current density $J(\boldsymbol{x}, t) = -\frac{1}{\tau} P(\boldsymbol{x}, t)\boldsymbol{x} - \frac{g}{2} \boldsymbol{\nabla} P$, we can rewrite (3.1) as

$$\frac{\partial P(\boldsymbol{x}, t)}{\partial t} + \boldsymbol{\nabla} \cdot \boldsymbol{J}(\boldsymbol{x}, t) = -\omega(\boldsymbol{x}, t) P(\boldsymbol{x}, t), \tag{3.2}$$

with the immediate consequence that, integrating both the LHS and the RHS over a ball B_R of radius R,

$$\begin{aligned} & \frac{d}{dt} \int_{B_R} P(\boldsymbol{x}, t) \mathrm{d}\boldsymbol{x} + \int_{B_R} \boldsymbol{\nabla} \cdot \boldsymbol{J}(\boldsymbol{x}, t) \mathrm{d}\boldsymbol{x} = -\int_{B_R} \omega(\boldsymbol{x}, t) P(\boldsymbol{x}, t) \mathrm{d}\boldsymbol{x} \\ \implies & \frac{d}{dt} \int_{B_R} P(\boldsymbol{x}, t) \mathrm{d}\boldsymbol{x} + \int_{\partial B_R} \boldsymbol{J}(\boldsymbol{x}, t) \cdot \mathrm{d}\boldsymbol{\Sigma} = -\int_{B_R} \omega(\boldsymbol{x}, t) P(\boldsymbol{x}, t) \mathrm{d}\boldsymbol{x} \\ \implies & \frac{d}{dt} S(t) = -\int_{\Omega} \omega(\boldsymbol{x}, t) P(\boldsymbol{x}, t) \mathrm{d}\boldsymbol{x}. \end{aligned} \tag{3.3}$$

In the second equality we have used Stoke's theorem whereas in the last we take the limit $R \to \infty$ and define the survival probability $S(t)$ of not being in the absorbing state as $\int P(\boldsymbol{x}, t)\mathrm{d}\boldsymbol{x}$. Accordingly, we shall define the absorption probability density $\phi(t)$ by

$$\phi(t) \equiv -\frac{\partial S(t)}{\partial t} \tag{3.4}$$

Dirichlet boundary conditions may be considered a particular case of the preceding construction by considering Ω to be the boundary and taking

$$\omega(\boldsymbol{x}) = \eta \int_{\Omega} \delta^{(2)}(\boldsymbol{x} - \boldsymbol{a})\mathrm{d}\boldsymbol{a} \tag{3.5}$$

for a constant η, where $\delta^{(n)}$ represents the n-dimensional Dirac delta function. To clearly understand what effective boundary condition this represents, it is useful to look at a one-dimensional example with a zero-dimensional (i.e. point) boundary. There, $\omega(x) = \eta\delta(x - a)$, and the equation would be

$$\frac{\partial}{\partial t}P(x,t) = \frac{g}{2}\frac{\partial^2}{\partial x^2}P(x,t) + \frac{1}{\tau}\frac{\partial}{\partial x}(xP(x,t)) - \eta\delta(x-a)P(x,t). \tag{3.6}$$

We integrate either side of the equation and impose continuity of $P(x,t)$, but not necessarily its derivative. At a in particular P can have only one-sided derivatives $P'_{>}(a)$ approaching from the right and $P'_{<}(a)$ from the left. As such,

$$\begin{aligned}
&\lim_{\epsilon\to 0^+}\int_{a-\epsilon}^{a+\epsilon} dx\left[\frac{g}{2}\frac{\partial^2 P}{\partial x^2} + \frac{1}{\tau}\frac{\partial}{\partial x}\left(xP(x,t)\right) - \eta\delta(x-a)P(x,t)\right] = 0\\
&\implies \frac{g}{2}\left[P'_{>}(a,t) - P'_{<}(a,t)\right] - \eta\langle P(a,t) = 0\\
&\implies P(a,t) = \frac{g}{2\eta}\left[P'_{>}(a,t) - P'_{<}(a,t)\right].
\end{aligned} \tag{3.7}$$

In the general case, one may define an inner solution $P_{<}(\boldsymbol{x}, t)$ and an outer solution $P_{>}(\boldsymbol{x}, t)$ to the boundary. These two solutions are "glued" at the boundary according to the condition set by $\omega(\boldsymbol{x})$. We proceed by integrating in a "Gaussian pillbox" [20] around any given point $\boldsymbol{b}$, to find

$$\frac{g}{2}\boldsymbol{\nabla}\left[P_{>}(\boldsymbol{x},t) - P_{<}(\boldsymbol{x},t)\right]\cdot\boldsymbol{n_b} = \eta P(\boldsymbol{b}), \tag{3.8}$$

where $\boldsymbol{n_b}$ is a unit vector normal to the surface at $\boldsymbol{b}$. Both in (3.7) and (3.8) we can see that Dirichlet boundary conditions at Ω are recovered for $\eta \to \infty$. For a general

value of η, we obtain again something analogous to the interface conditions for an electric field across a charged surface.

3.2 The road problem

With the "leaky" FPE defined as in the previous section, we're fully equipped to pose a model for interactions across a linear domain, which we'll simply refer to as a "road" R. Assuming the individual moves isotropically about its home-range, there is no loss of generality in considering the road, at a distance a from the home-range center, to be represented by the line $R = \{\boldsymbol{x} \in \mathbb{R}^2 | x_1 = a\}$ in the plane $\mathbb{R}^2 = \{(x_1, x_2) \in \mathbb{R} \times \mathbb{R}$. "Morally", the situation we want to represent is one where the trajectory of the focal individual is described by a set of rules

$$\text{(i) } \mathrm{d}\boldsymbol{x} = -\frac{\boldsymbol{x}}{\tau}\mathrm{d}t + \sqrt{g}\mathrm{d}\boldsymbol{W}_t \tag{3.9}$$

$$\text{(ii) Whenever } \boldsymbol{x}(t) \text{ crosses } R\text{, end the process with probability } P_a. \tag{3.10}$$

As we will discuss later in this chapter, the "Markov process" described above is not well posed for $0 < P_a < 1$, and a proper formulation of the situation above requires some technical care. Intuitively, nonetheless, we expect this is the microscopic description of a process that should have, as a master equation, the "leaky" FPE (3.1) with $\omega((x), t) = \eta\delta^{(1)}(x_1 - a)$. Because of the assumption that the process is isotropic, symmetry dictates the x_2 variable cannot influence the absorption time. Thus, along the $x \equiv x_1$ direction, the macroscopic equation is simply (3.6).

The remaining variable $y \equiv x_2$ will simply follow the previous equation with boundary conditions at infinity, so the absorption position along the y coordinate will simply follow the PDF of the "free" process. That is to say, the absorption probability density for deterministic initial conditions should factorize as

$$\phi_{(a,y)}(t|x_0, y_0) = \phi_a(t|x_0)P(y, t|y_0) \tag{3.11}$$

Note, therefore, that the evolution of the survival rate simply becomes

$$\frac{d}{dt}S(t) = -\eta P(a, t). \tag{3.12}$$

In the limit of $\eta \to \infty$, the road problem simply becomes the first-passage problem

for a 1D OU process. We shall review this problem, and then derive some results for a general value of η.

3.2.1 Mean first-absorption time for the road problem

Since the process described by the master equation (3.6) is time-homogeneous and satisfies the Markov property, the transition probability $P(x,t|x_0)$ obeys the backwards equation

$$\frac{\partial}{\partial t}P(x,t|x_0) = \frac{g}{2}\frac{\partial^2}{\partial x_0^2}P(x,t|x_0) - \frac{x_0}{\tau}\frac{\partial}{\partial x_0}P(x,t|x_0) - \eta\delta(x_0-a)P(x,t|x_0). \quad (3.13)$$

We start at the more familiar case of $\eta \to +\infty$. We can investigate an initial-value problem for $S(t) \equiv \int P(\boldsymbol{x},t)\mathrm{d}\boldsymbol{x}$. Initially, $S(t=0|x_0) = 1$. Furthermore, $S(t|a) = 0$, since a is a perfectly absorbing boundary. To fully specify an initial-value problem, we need to impose one further condition. One way of doing it, which will allow for comparisons with reflected Brownian motion, is imposing reflecting boundaries at two points $b_\pm$ such that $b_- < a < b_+$. We can now solve the equation on two domains, namely $[b_-, a]$ and $[a, b_+]$, with $\partial_{x_0} S_\pm(t|x_0)|_{x_0=b_\pm} = 0$, meaning no flux remains at the boundary — reflection. To obtain the solution for an unbounded domain, it suffices to consider the limit $b_\pm \to \pm\infty$. As such, the ODE for the the mean first-passage time will be

$$\begin{aligned} &L^\dagger\langle T\rangle_a(x_0) = -1, \\ &\langle T\rangle_a(a) = 0, \\ &\langle T\rangle_a'(b_\pm) = 0, \end{aligned} \quad (3.14)$$

where $L = \frac{g}{2}\partial_x^2 + \frac{1}{\tau}\partial_x$, and again the no-flux boundary conditions at $\pm b$ are due to reflection at these points. We can solve this initial value problem by elementary means: the full solution is a sum of a particular solution to the inhomogeneous equation with the general solution of the homogeneous equation. Free parameters are fixed by the boundary conditions. We start solving (3.14) by solving the associated homogeneous equation ($L^\dagger\langle T\rangle_{HOM,a} = 0$) by separation of variables,

$$\frac{\langle T\rangle''_{HOM,a}(x_0)}{\langle T\rangle'_{HOM,a}(x_0)} = \frac{2x_0}{g\tau} \tag{3.15}$$

$$\implies \int^{x_0} \frac{\langle T\rangle''_{HOM,a}(x)}{\langle T\rangle'_{HOM,a}(x)} dx = \log\left(\frac{\langle T\rangle'_{HOM,a}(x_0)}{c_1}\right) = \frac{x_0^2}{g\tau} \tag{3.16}$$

$$\implies \langle T\rangle_{HOM,a}(x_0) = c_0 + \frac{\sqrt{\pi g\tau}}{2} c_1 \mathrm{erfi}\left(\frac{x_0}{\sqrt{g\tau}}\right) \tag{3.17}$$

for some real constants c_0 and c_1. We make use of the error functions erf and erfi defined as

$$\mathrm{erf}(x) \equiv \frac{2}{\sqrt{\pi}} \int_0^x \exp\left(-x^2\right) \mathrm{d}x, \tag{3.18}$$

$$\mathrm{erfi}(x) \equiv -i\mathrm{erf}(-ix) = \frac{2}{\sqrt{\pi}} \int_0^x \exp\left(x^2\right) \mathrm{d}x. \tag{3.19}$$

All that remains is to find a particular solution $\langle T\rangle_{0,a}(x_0)$ to the inhomogeneous equation, which is again possible by elementary means, using an integration factor of $\exp\left(-x^2/g\tau\right)$:

$$\frac{d}{dx_0}\left[\exp\left(-\frac{x^2}{g\tau}\right)\langle T\rangle'_{0,a}(x_0)\right] = -\frac{2}{g}\exp\left(-\frac{x^2}{g\tau}\right) \tag{3.20}$$

$$\implies \langle T\rangle'_{0,a}(x_0) = -\sqrt{\frac{\pi\tau}{g}}\exp\left(\frac{x^2}{g\tau}\right)\mathrm{erf}\left(\frac{x}{\sqrt{g\tau}}\right) \tag{3.21}$$

$$\implies \langle T\rangle_{0,a}(x_0) = -\frac{x_0^2}{g}{}_2F_2\left(1,1;\frac{3}{2},2;\frac{x_0^2}{g\tau}\right), \tag{3.22}$$

where the last integration in terms of the generalized hypergeometric function ${}_pF_q$ is given by Mathematica. The full solution is thus given by $\langle T\rangle_a(x_0) = \langle T\rangle_{0,a}(x_0) + \langle T\rangle_{HOM,a}(x_0)$ with the initial conditions provided by (3.14), which impose

$$\begin{cases} \langle T\rangle_a(a) & = c_0 + \frac{\sqrt{\pi g\tau}}{2} c_1 \mathrm{erfi}\left(\frac{a}{\sqrt{g\tau}}\right) - \frac{a^2}{g}{}_2F_2\left(1,1;\frac{3}{2},2;\frac{a^2}{g\tau}\right) = 0 \\ \langle T\rangle'_a(b_\pm) & = c_1 \exp\left(\frac{b_\pm^2}{g\tau}\right) - \sqrt{\frac{\pi\tau}{g}}\exp\left(\frac{b_\pm^2}{g\tau}\right)\mathrm{erf}\left(\frac{b_\pm}{\sqrt{g\tau}}\right) =, \end{cases} \tag{3.23}$$

which, solving for c_0 and c_1, imply the solutions on the half-domains to be

$$\begin{aligned}\langle T\rangle_{\pm,a}(x_0) = \frac{\pi}{2}\tau\mathrm{erf}\left(\frac{b_\pm}{\sqrt{g\tau}}\right)\left[\mathrm{erfi}\left(\frac{x_0}{\sqrt{g\tau}}\right) - \mathrm{erfi}\left(\frac{a}{\sqrt{g\tau}}\right)\right] \\ - \left(\frac{x_0^2}{g}{}_2F_2\left(1,1;\frac{3}{2},2;\frac{x_0^2}{g\tau}\right) - \frac{a^2}{g}{}_2F_2\left(1,1;\frac{3}{2},2;\frac{a^2}{g\tau}\right)\right).\end{aligned} \tag{3.24}$$

With this, all that remains for the solution on the entire domain is to take the limits $b_\pm \to \pm\infty$. While for an actual one dimensional problem this is entirely optional — this is the exact solution of the mean first-passage time of one-dimensional OU motion in a domain with absorption at a [21, 22, 23, 24] and reflection at $\pm b$, for use in the two-dimensional problem we want to restore the polar symmetry of the full domain. Noting $\mathrm{erf}(\pm\infty) = \pm 1$, we have

$$\begin{aligned}\langle T\rangle_a(x_0) = \frac{\pi}{2}\tau\left|\mathrm{erfi}\left(\frac{a}{\sqrt{g\tau}}\right) - \mathrm{erfi}\left(\frac{x_0}{\sqrt{g\tau}}\right)\right| \\ + \sqrt{\frac{\pi\tau}{g}}\int_{x_0}^{a}\exp\left(\frac{x^2}{g\tau}\right)\mathrm{erf}\left(\frac{x}{\sqrt{g\tau}}\right)\mathrm{d}x.\end{aligned} \tag{3.25}$$

This result is not easy to interpret at a first glance. For a sanity check, we may begin by noting erf is a bounded sigmoidal function that takes on values in the interval $[-1,1]$. This guarantees that the first term in the RHS of (3.25) dominates the second in absolute value. Intuitivelly, this tells us that initial conditions on the side of the road opposite the home-range center are shorter-lived than their reflections about the road. To understand the quantitative behavior of the solution, we can begin by analyzing its asymptotic properties.

3.2.2 Asymptotics for $\langle T\rangle_a(x_0)$

Suppose the road is "placed" at a large distance from the animal's home range, that is $a \gg 0$. From (3.25) it is clear that one needs asymptotic expansions for the error functions. As discussed, for $x_0 \gg 0$,

$$\begin{aligned}\sqrt{\frac{\pi\tau}{g}}\int_0^{x_0}\exp\left(\frac{x^2}{g\tau}\right)\mathrm{erf}\left(\frac{x}{\sqrt{g\tau}}\right)dx \sim_{x_0\gg 0} \sqrt{\frac{\pi\tau}{g}}\int_0^{x_0}\exp\left(\frac{x^2}{g\tau}\right)dx \\ = \frac{\pi}{2}\tau\mathrm{erfi}\left(\frac{x_0}{\sqrt{g\tau}}\right).\end{aligned} \tag{3.26}$$

This confirms the argument that the fast-growing x_0 dependent terms in (3.25) asymptotically cancel out. This leaves behind only a slow growth in x_0. We can expand $\mathrm{erf}(z)$ via iterative integration by parts:

$$\begin{aligned}
\mathrm{erf}(z) &= \frac{2}{\sqrt{\pi}} \int_0^z \exp\left(x^2\right) dx \\
&= \frac{2}{\sqrt{\pi}} \left(\int_0^\infty \exp\left(x^2\right) dx - \int_z^\infty \exp\left(x^2\right) dx \right) \\
&= 1 - \frac{2}{\sqrt{\pi}} \int_z^\infty \exp\left(x^2\right) dx \\
&= 1 - \frac{2}{\sqrt{\pi}} \left(-\frac{\exp\left(x^2\right)}{2x} \bigg|_z^\infty - \int_z^\infty \frac{\exp\left(x^2\right)}{2x^2} \right) \\
&= 1 - \frac{2}{\sqrt{\pi}} \left(\frac{\exp\left(-z^2\right)}{2z} - \frac{\exp\left(-z^2\right)}{4z^3} + \int_z^\infty \frac{3\exp\left(x^2\right)}{4x^4} \right) \\
&= 1 - \frac{\exp\left(-z^2\right)}{\sqrt{\pi}} \sum_{n=0}^{\infty} \frac{(-1)^n (2n-1)!!}{2^n z^{2n+1}}.
\end{aligned} \tag{3.27}$$

Using this last expansion in the expression for $\langle T \rangle_a(x_0)$,

$$\begin{aligned}
&\sqrt{\frac{\pi\tau}{g}} \int_{x_0}^a \exp\left(\frac{x^2}{g\tau}\right) \mathrm{erf}\left(\frac{x}{\sqrt{g\tau}}\right) \mathrm{d}x \\
&\quad = \left[\frac{\pi}{2} \tau \mathrm{erfi}\left(\frac{x}{\sqrt{g\tau}}\right) \right]_{x_0}^a + \tau \sum_{n=0}^{\infty} \frac{(-1)^n (2n-1)!!}{2^n} \int_{x_0/\sqrt{g\tau}}^{a/\sqrt{g\tau}} \frac{\mathrm{d}u}{u^{2n+1}} \\
&\quad = \frac{\pi}{2} \tau \left[\mathrm{erfi}\left(\frac{a}{\sqrt{g\tau}}\right) - \mathrm{erfi}\left(\frac{x_0}{\sqrt{g\tau}}\right) \right] + \tau \log\left(\frac{x_0}{a}\right) \\
&\quad + \left[\sum_{n=1}^{\infty} \frac{(-1)^n (2n-1)!!}{2^{n+1} n} \left(\frac{x^2}{g\tau}\right)^{-n} \right]_{x_0}^a
\end{aligned} \tag{3.28}$$

Similarly, for $x_0 \ll a$, we'll have to adopt the same expansion (3.27), but with all signs reversed, after all erf is an odd function. The conclusion:

$$\langle T \rangle_a(x_0) = \pi\tau \mathrm{erfi}\left(\frac{a}{\sqrt{g\tau}}\right) \theta_H\left(\frac{a - x_0}{\sqrt{g\tau}}\right) + \tau \log\left|\frac{x_0}{a}\right| + \mathcal{O}\left(x_0^{-2}\right). \tag{3.29}$$

with θ_H the Heaviside theta function. While this result is correct asymptotically, this can be hard to verify numerically because $\mathrm{erf}(x)$ has problematic numerical

convergence. A better approximation is to take $x_0 \mapsto (x_0 - a)$ in (3.29), so that the shape of the original function is respected, and the asymptotic convergence can be numerically verified in Figure 3.1.

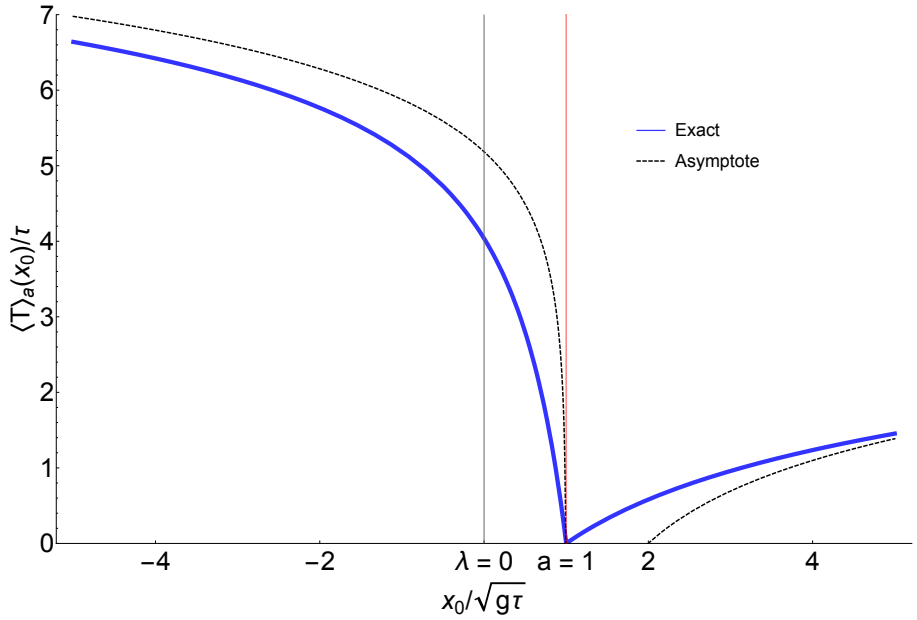

Figure 3.1: Asymptotic convergence of 3.29 to the MFPT

3.2.3 Finite η

We now move on to the case where η is a finite quantity. Thus, our initial value problem becomes

$$\begin{aligned}(L^\dagger - \eta\delta(x_0 - a))\langle T\rangle_a(x_0) &= -1,\\ \langle T\rangle_a'(b_\pm \to \pm\infty) &= 0.\end{aligned} \tag{3.30}$$

We split the domains into $[-\infty, a)$ and $(a, \infty]$, and we know inside each one of them that $\delta(x_0 - a) \equiv 0$, so that the general form of the solutions $\langle T\rangle_{\pm,a}(x_0)$ is, as we calculated before,

$$\langle T\rangle_{\pm,a}(x_0) = c_{0\pm} \pm \frac{\pi\tau}{2}\text{erfi}\left(\frac{x_0}{\sqrt{g\tau}}\right) + \sqrt{\frac{\pi\tau}{g}}\int_{x_0}^{a}\exp\left(\frac{x^2}{g\tau}\right)\text{erf}\left(\frac{x}{\sqrt{g\tau}}\right)\mathrm{d}x. \tag{3.31}$$

The determination of the constants $c_{0\pm}$ is done by imposing the condition of discontinuity of the first derivative, which is derived identically to (3.8).

Plugging our known solutions (3.31) into the boundary discontinuity condition, we find

$$\langle T\rangle_a(a) = \frac{\sqrt{\pi g\tau}}{\eta}\exp\left(\frac{a^2}{g\tau}\right). \tag{3.32}$$

Finally, we can write the full solution

$$\begin{aligned}\langle T\rangle_a(x_0) = \frac{\sqrt{\pi g\tau}}{\eta}\exp\left(\frac{a^2}{g\tau}\right) + \frac{\pi}{2}\tau\left|\operatorname{erfi}\left(\frac{a}{\sqrt{g\tau}}\right) - \operatorname{erfi}\left(\frac{x_0}{\sqrt{g\tau}}\right)\right| \\ + \sqrt{\frac{\pi\tau}{g}}\int_{x_0}^{a}\exp\left(\frac{x^2}{g\tau}\right)\operatorname{erf}\left(\frac{x}{\sqrt{g\tau}}\right)\mathrm{d}x.\end{aligned} \tag{3.33}$$

We can conclude therefore that the relaxation to partial absorption amounts to adding a term to the solution of the perfectly absorbing boundary, which goes inversely with the absorption parameter η. In particular, we can verify that the previous case is obtained in the limit $\eta \to +\infty$.

3.2.4 The brownian limit

To finalize the analysis, we demonstrate how one should retrieve Brownian motion from the OU model in the limit $\tau \to +\infty$. This is not entirely trivial, as Brownian motion in an infinite region has unbounded variance. Thus, in the Brownian case one needs to preserve reflecting boundaries, which also means the corresponding two-dimensional problems in fact have different symmetries — the Brownian domain is going to be a rectangle in 2D. Note that, as $\tau \to \infty$,

$$\begin{aligned}&\sqrt{\frac{\pi\tau}{g}}\int_{x_0}^{a}\exp\left(\frac{x^2}{g\tau}\right)\operatorname{erf}\left(\frac{x}{\sqrt{g\tau}}\right)\mathrm{d}x \\ &\quad= 2\sqrt{\frac{\tau}{g}}\int_{x_0}^{a}\left[1+\mathcal{O}\left(\tau^{-1}\right)\right]\left[\frac{x}{\sqrt{g\tau}}+\mathcal{O}\left(\tau^{-3/2}\right)\right]\mathrm{d}x \\ &\quad= \frac{a^2}{g} - \frac{x_0^2}{g} + \mathcal{O}\left(\tau^{-1}\right).\end{aligned} \tag{3.34}$$

Similarly,

$$\operatorname{erfi}\left(\frac{x_0}{\sqrt{g\tau}}\right) = \frac{2x_0}{\sqrt{\pi g\tau}} + \mathcal{O}\left(\tau^{-3/2}\right). \tag{3.35}$$

We can insert these expansions into $\langle T\rangle_a(x_0)$ to conclude that

$$\langle T\rangle_a(x_0) = \frac{\sqrt{\pi g\tau}}{\eta} + \sqrt{\frac{\pi\tau}{g}}|x_0 - a| + \frac{a^2}{g} - \frac{x_0^2}{g} + \mathcal{O}\left(\tau^{-1/2}\right). \tag{3.36}$$

This suggests that, introducing some time scale τ_{eff} via symmetric reflecting boundaries conditions, the mean first absorption time for Reflected Brownian motion (RBM) should have the functional form

$$\langle T^{\text{B}}\rangle_a(x_0) = \frac{\sqrt{\pi g\tau_{\text{eff}}}}{\eta} + \sqrt{\frac{\pi\tau_{\text{eff}}}{g}}|x_0 - a| + \frac{a^2}{g} - \frac{x_0^2}{g}. \tag{3.37}$$

We can of course calculate the aforementioned quantity directly from an initial value problem, namely,

$$\begin{aligned} \frac{g}{2}\langle T^{\text{B}}\rangle_a''(x_0) - \eta\delta(x_0 - a) &= -1 \\ \langle T^{\text{B}}\rangle_a'(\pm b) &= 0. \end{aligned} \tag{3.38}$$

From the above equation it is immediate that the solution has to be composed of two quadratic functions which are "soldered" at the point a. More directly, we can verify that

$$\langle T^{\text{B}}\rangle_a(x_0) = \frac{2b}{\eta} + \frac{2b}{g}|x_0 - a| + \frac{a^2}{g} - \frac{x_0^2}{g}, \tag{3.39}$$

and thus arrive exactly at (3.37) by imposing $b = \sqrt{\pi g\tau_{\text{eff}}}/2$. The necessity of introducing the cut-off point b to the domain makes it harder to compare the OU and Brownian cases. We may set the operational definition of a home-range to be the region delimited by the 95th percentile of the stationary spatial distribution of an individual animal. Under this convention, the natural choice would be $b = K_{95\%}\sqrt{g\tau} \equiv \sqrt{-\log(1 - 0.95)g\tau}$. It is hard to separate out regimes in which Brownian motion can provide a good estimate of the mean absorption. Under uncertainty about the initial condition (that is, in the case where x_0 is sampled

from some non-trivial distribution), it can over or underestimate (Figs. 3.2, 3.3) the "truer" value derived considering OU processes. In general, the lack of a center of attraction makes it so that Brownian motion effectively "runs off" randomly in situations where drift in the OU process continually pushes systems towards one particular point in space.

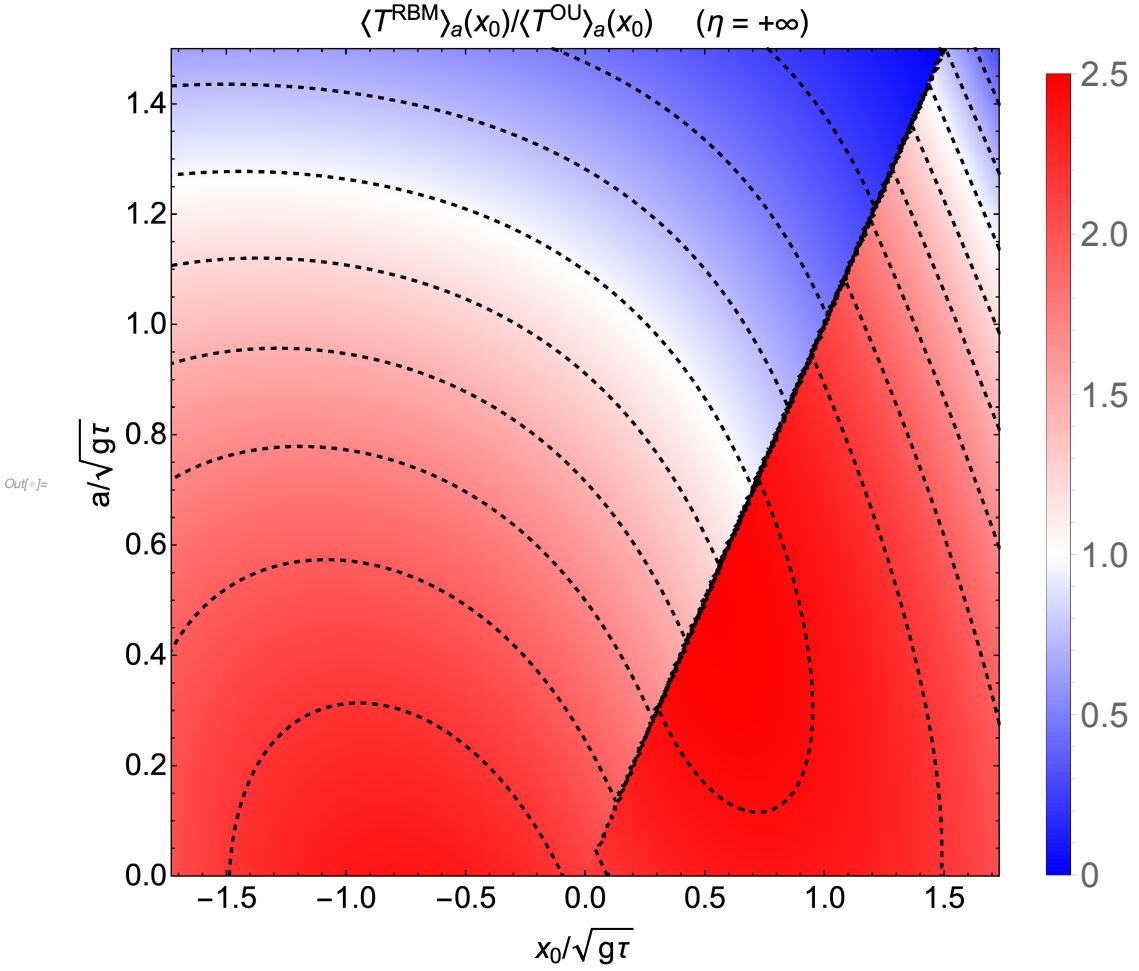

Figure 3.2: Heat maps of the quotient between the RBM and the OU mean absorption times for $\eta \to +\infty$.

3.3 Determining η and Simulations

A crucial step to connect the theory developed so far in this chapter and data is the ability, in principle, to derive the parameters of the problem from time-series. The parameters of pure OU motion all have a very clear interpretation in terms of length and time scales, making it useful in accurately estimating

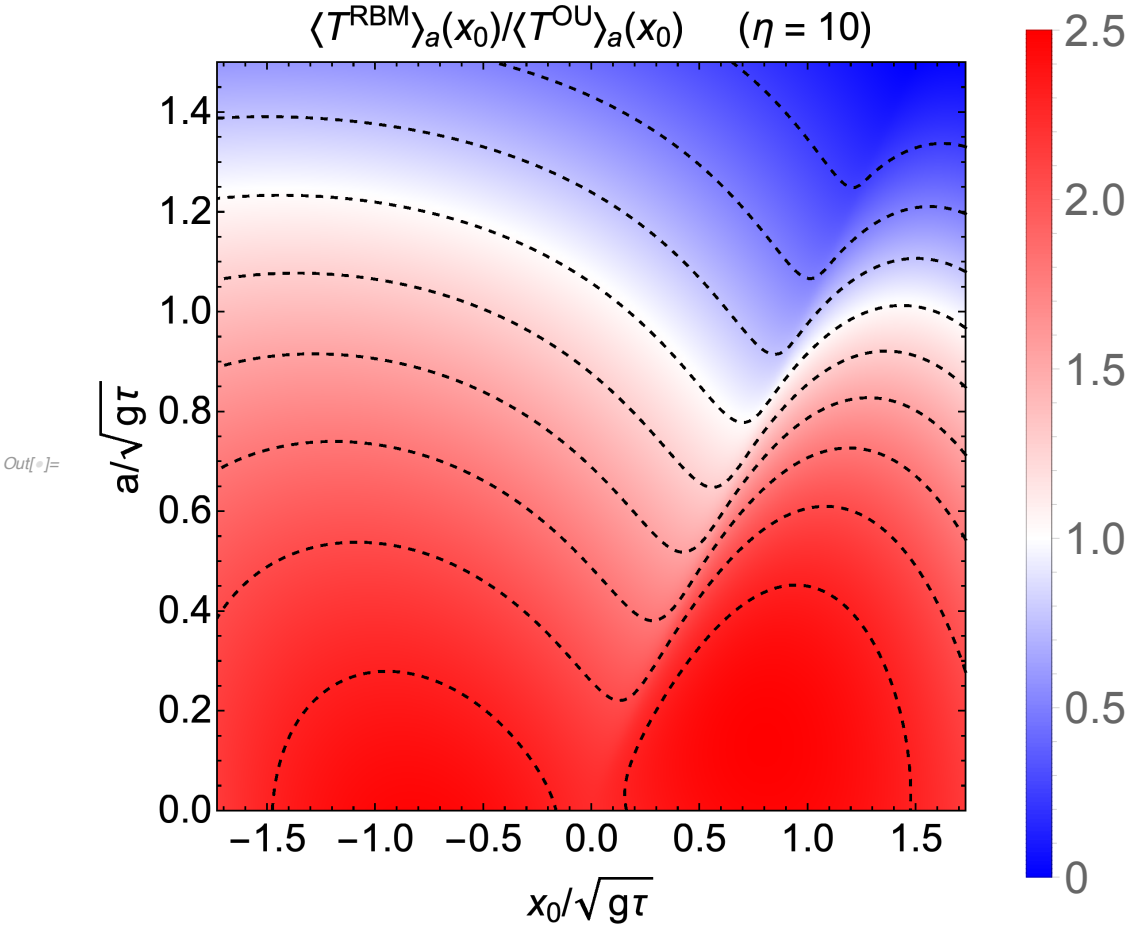

Figure 3.3: Heat maps of the quotient between the RBM and the OU mean absorption times for $\eta = 10$.

home-ranges [14] from tracking data. The absorption rate parameter η remains somewhat mysterious when it comes to microscopic properties of trajectories. It has dimensions of velocity, but in 3.39 it is not clear what this velocity would be associated to, as it is a ratio between the size of the domain and the first absorption time starting at the road itself ($\langle T^{\mathrm{B}} \rangle_a(a)$).

We conjectured, at the start of the chapter, that the probability distribution in an equation with partial absorption such as (3.30) should be equivalent to a Markov process (3.9) which is absorbed with some fixed probability P_a whenever it hits the semi-absorbing boundary. As such, a physical interpretation of η would involve connecting it to such a probability P_a. It is however, not possible to make this association. Since Brownian motion is almost-surely nowhere differentiable, the fractal-like nature of the trajectory precludes one from counting the number of intersections between a realization and a given domain of codimension one.

More explicitly, counting crossings would require approximating the trajectory at the boundary by a line segment, but since the solution of the associated stochastic differential equation is non-differentiable, this is by definition not possible.

To show the issue more clearly, we may begin by integrating 3.9 via an Euler scheme with time-step Δt. This is exactly the procedure we use to solve these stochastic differential equations numerically. One obtains a jump process described by the forward Kolmogorov equation for its probability distribution $p_{\Delta t}(x,t)$. We may simply impose the absorption condition P_a upon crossing the boundary at a, yielding

$$\begin{aligned} p_{\Delta t}(x,t+\Delta t)|_{x>a} = &\int_a^\infty \frac{p_{\Delta t}(y,t)}{\sqrt{2\pi g \Delta t}} \exp\left[-\frac{(x-y-y\Delta t/\tau)^2}{2g\Delta t}\right] \mathrm{d}y \\ &+ (1-P_a)\int_{-\infty}^a \frac{p_{\Delta t}(y,t)}{\sqrt{2\pi g \Delta t}} \exp\left[-\frac{(x-y-y\Delta t/\tau)^2}{2g\Delta t}\right] \mathrm{d}y, \end{aligned} \tag{3.40}$$

$$\begin{aligned} p_{\Delta t}(x,t+\Delta t)|_{x<a} = &(1-P_a)\int_a^\infty \frac{p_{\Delta t}(y,t)}{\sqrt{2\pi g \Delta t}} \exp\left[-\frac{(x-y-y\Delta t/\tau)^2}{2g\Delta t}\right] \mathrm{d}y \\ &+ \int_{-\infty}^a \frac{p_{\Delta t}(y,t)}{\sqrt{2\pi g \Delta t}} \exp\left[-\frac{(x-y-y\Delta t/\tau)^2}{2g\Delta t}\right] \mathrm{d}y. \end{aligned} \tag{3.41}$$

It is known [25] that for Brownian motion, the absorption flux at the boundary a diverges as $1/\sqrt{\Delta t}$. This result must be preserved for OU motion as well, since the corrections of any drift term only appear at order Δt in the equation, leaving the Wiener portion (which contributes with the terms of order $\sqrt{\Delta t}$) of the process unaffected. More intuitively, the correction of any drift term is a deterministic contribution that does not affect the non-differentiable behavior of the trajectory. This is a particularly key observation, as it means that to study the local behavior of the Euler approximation at the semi-absorbing boundary there is no loss of generality in considering simple Brownian motion. Since the number of crossings increases with $1/\sqrt{\Delta t}$, for arbitrarily small Δt the absorption probability in any given crossing goes to unity **regardless of the value of** P_a. The immediate consequence is that the probability distribution in the previous two equations will converge, as $\Delta t \to 0$, to the solutions of the Fokker-Planck equation with Dirichlet boundary conditions, leading to equation (3.14) for the mean first-passage time.

The upshot of this exposition is that, if a connection between η and some kind

of discrete absorption probability P_a is to be derived, a precise scaling of P_a with Δt must be established. This is not a failure of the model, as we can imagine in nature Δt is indeed some characteristic scale of the problem — animals do not move in infinitely tortuous trajectory, so at some temporal resolution we start observing ballistic segments of motion. Furthermore, data itself will inevitably come with a Δt. From this point of view, the link between the probability of absorption and the time-scale becomes quite natural, and we can claim the discrete process is the more realistic model which we approximate by a continuous one to leverage the power of the theory developed so far (at the cost of introducing a parameter, η).

3.3.1 Analogy with Robin boundary conditions

A very similar problem to the one we are running into has been analyzed in a slightly different context. Descriptions of random movement subject to partially *reflecting* boundaries employ the so-called Robin or radiation boundary conditions. For example, a stochastic process macroscopically described by a Fokker-Planck equation with Fokker-Planck operator L and semi-reflecting boundaries at $x = 0$ might be described by

$$\begin{aligned} \frac{\partial P}{\partial t} &= LP \\ -J(0,t) &= \kappa P(0,t) \end{aligned} \tag{3.42}$$

with $J(x,t)$ the probability current. In the case of Brownian processes, this reduces to

$$\frac{g}{2}\frac{\partial P}{\partial x}\Big|_{x=0} = \kappa P(0). \tag{3.43}$$

For Brownian motion, a process subject to Robin boundary conditions or to a boundary flux discontinuity condition (3.8) should have the exact same behavior. This is a consequence of the space-homogeneity of the Wiener process — whenever the partially permeable boundary is crossed, one may equivalently look at its specular reflection about the boundary as a realization of the partially reflected process. This immediately leads to the identification $\kappa \leftrightarrow \eta/2$. As with the situation above, the partially absorbing boundary problem has a representation $p_{\Delta t}^{PR}$ in terms of the Euler-Maruyama method. Taking $a = 0$ without loss of generality

$$p^{PR}_{\Delta t}(x, t+\Delta t) = \int_0^\infty \frac{p^{PR}_{\Delta t}(y,t)}{\sqrt{2\pi g \Delta t}} \Bigg\{ \exp\left[-\frac{(x-y)^2}{2g\Delta t}\right] + (1-P_a)\exp\left[-\frac{(x+y)^2}{2g\Delta t}\right] \Bigg\} \mathrm{d}y. \tag{3.44}$$

One can proceed with a careful analysis of the previous equation [26, 27]. There are a few important results, mostly revolving around the non-uniform convergence of $p^{PR}_{\Delta t}(x,t)$ to the solution of the Fokker-Planck equation (3.42) as $\Delta t \to 0$ around the boundary point, in such a way that the operation of taking $\kappa \to +\infty$ does not commute with many operations on the discretized system. What is proposed instead is to conduct a so-called **boundary layer analysis**, which involves a careful order-by-order (in $\sqrt{\Delta t}$) analysis of the properties of the appropriately rescaled discrete system around the bounary point a. What this reveals is that, even including a general drift term to the dynamics — quite analogously to how we argued above, one can derive a general relation between the time-step reescaled absorption probability $P_a \equiv P_0\sqrt{\Delta t}$ and the absorption rate κ. This ends up being

$$\kappa = \sqrt{\frac{g}{2\pi}} P_0 \iff \eta = \sqrt{\frac{2g}{\pi}} P_0. \tag{3.45}$$

3.3.2 Simulations

Combining the arguments we have made previously, since **(i)** locally around the boundary only the diffusive portion needs to be considered and **(ii)** there is a mapping between the boundary behavior of partially permeable boundaries and partially reflecting boundaries, we find the relationship (3.45) should hold for any process with drift and constant diffusion. We may verify this by estimating the value of η independently from simulations. This is done by simply simulating the associated Euler process. Integrating (3.9) on a finite time interval Δt, we can write [28]

$$x(0) = x_0 \tag{3.46}$$

$$x(t+\Delta t) = x(t)\exp(-\Delta t/\tau) + \sqrt{\frac{g\tau}{2}(1-\exp(-2\Delta t/\tau))}\, u_t \tag{3.47}$$

where all the $u_t \sim \mathcal{N}(0,1)$ are identically independently distributed standard normal variables.

There is no loss of generality in normalizing to unity the spatial and temporal scales by setting $g = \tau = 1$. Then, for each initial condition x_0, value of the scaled absorption probability P_0 and road position a, we produce a large number N (10^5) of realizations of the Euler scheme for the process. Each realization i will be associated with an observed absorption time $T_i(x_0)$. We define our simulation mean first absorption time as the sample mean of these observations

$$\langle T \rangle_a^{\text{Sim}}(x_0) = \frac{1}{N} \sum_{i=1}^{N} T_i(x_0). \tag{3.48}$$

We can now utilize a particular case of our analytical solution to produce a convenient identity connecting η to $\langle T \rangle_a$, namely

$$\langle T \rangle_a(a) = \frac{\sqrt{\pi g \tau}}{\eta} \exp\left(\frac{a^2}{g\tau}\right), \tag{3.49}$$

which motivates us to define

$$\eta^{\text{Sim}} \equiv \frac{\sqrt{\pi g \tau}}{\langle T \rangle_a^{\text{Sim}}(a)} \exp\left(\frac{a^2}{g\tau}\right). \tag{3.50}$$

We verify that, with this single data point $\langle T \rangle_a^{\text{Sim}}(a)$, we can use η^{Sim} to reliably extrapolate the complete range of $\langle T \rangle_a^{\text{Sim}}(x_0)$ throughout its domain (Fig 3.4). Furthermore, we verify that this estimate is in very close agreement with the theoretically predicted value of η (Fig 3.5), independently of the presence or absence of drift. More precisely, we verify the convergence to unity of η/η^{Sim} as a function of $\sqrt{\Delta t}$, with P_0 held fixed, with η given by (3.45).

3.4 Discussion and next steps

In this chapter, we have developed a general formalism for interactions with traversable features of a landscape. We then specialized it to a particularly simple system, which we were able to treat analytically. While the list of organisms whose behavior is well modeled by the "road problem" may be small — those whose movement patterns are not altered by the presence of a road being better candidates for model fit than others, the framework presented is very flexible. For animals who adapt their motion to the modified habitat, for example, movement

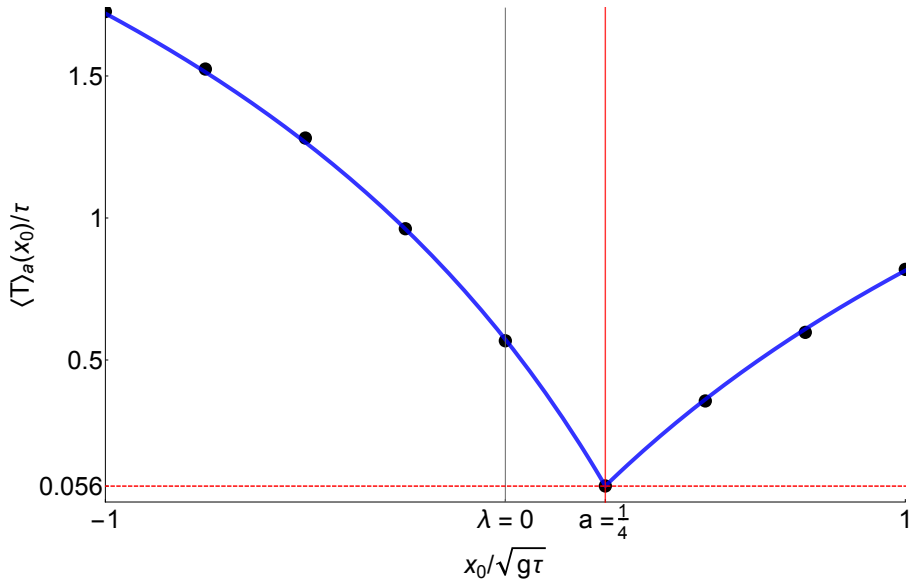

Figure 3.4: Example of simulation and analytical prediction of $\langle T \rangle_a(x_0)$ for $a = \sqrt{g\tau}/4$ and $P_a = 0.8$

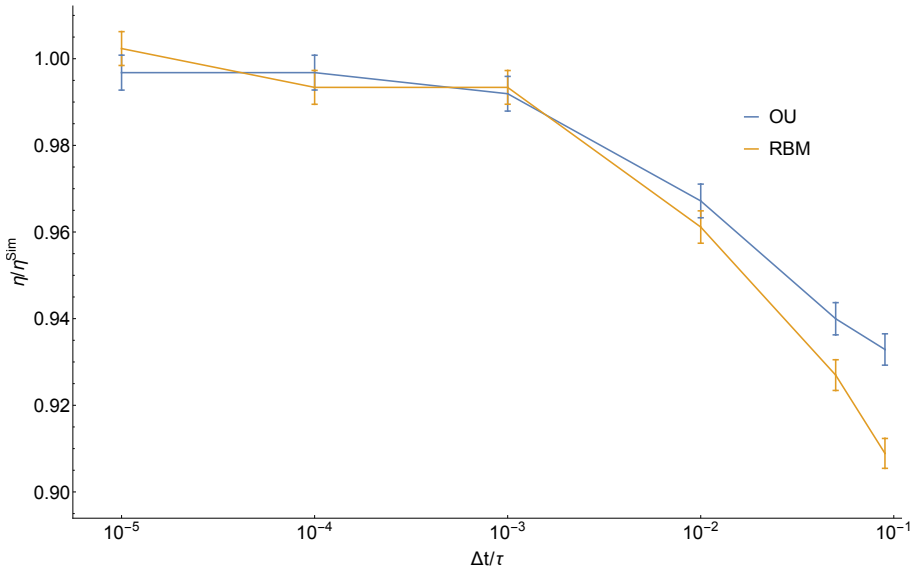

Figure 3.5: Convergence of simulated to theoretical value of η as function of the time step Δt

may be modeled by space-dependent drift and diffusion coefficients. The same may be done to produce simple models of terrain or vegetation inhomogeneity. A similar class of simple extensions would be those involving time dependent absorption rates, i.e., making $\eta = \eta(t)$. This again would be necessary to more accurately model e.g. the time inhomogeneous volume of traffic.

The approach here developed is quite general, and may serve as an important

step for rigorously formulating various ecological processes. It would be interesting, for example, to investigate optimization tasks involving minimization of accident risk given some spatial distribution of home-ranges. Even in situations where the interaction domain under consideration is not exactly linear, the linear domain at a distance a will necessarily give a lower bound for the first-interaction time with a geometry that has nearest approximation at that same distance a. Moving forward, the objective is to more clearly delimit clear examples of the techniques here developed in action. This would require analysis of, as shown previously, movement data for animals such as giant anteaters.

Chapter 4

Encounters between two home-ranging individuals

In the context of biological interactions and their scaled-up consequences at the level of population dynamics, a minority of what is done on the side of modelling explicitly considers movement. Motion is, nonetheless, one of the central ways by which animals explore and therefore interact with their surroundings. It ultimately underlies such basic processes as foraging, hunting, mate-finding, migration — and therefore modulation of gene flow. In particular, adaptation in movement behavior is key in understanding the evolution of ecological interactions [29, 30]. In light of all of this, it is quite attractive to have a mechanistic, quantitative description of processes mediated by movement.

This motivates the study of encounters between two (or more) animals, that is, events of close approximation between individuals. Encounters are by themselves often not a complete description of an interaction. For example, predation may involve chasing, territorial dispute may involve ritualized aggression, mate-finding may involve courtship displays, all of which often have themselves a component of movement. There are, furthermore, other means by which spatial interactions may happen without encounters, an example being scent-marking. Nonetheless, encounters are a way by which we can understand the minimal condition for the "triggering" of various kinds of interaction. Just as in the previous chapter, in the absence of a detailed description of a particular process of interest, we may treat the interaction itself as a discrete probabilistic event that may happen upon the two individuals coming close enough to one another.

In this chapter, we briefly sketch a theory of two-individual processes with encounter-dependent interactions. We will show that, even though the problem seems initially more complicated than the one studied in the previous chapter, it can be in fact treated as a particular case of that general framework. The mean first-interaction time of two identical individuals, a particularly symmetric case, is

solved analytically.

4.1 Defining encounters between individuals

Suppose we have two individuals described by trajectories $\boldsymbol{x}_i(t)$, $i = 1, 2$. The general problem we want to address is that of an interaction which may take place probabilitically upon these two individuals coming an interaction distance q of one another. That is, we desire to count events

$$\|\boldsymbol{x}_1(t) - \boldsymbol{x}_2(t)\| \leq q. \tag{4.1}$$

The natural impetus in this situation is to analyze the system utilizing relative coordinates. Indeed, one can look at the process defined in terms of

$$\begin{aligned} \boldsymbol{r} &= \boldsymbol{x}_1 - \boldsymbol{x}_2 \\ \boldsymbol{R} &= \boldsymbol{x}_1 + \boldsymbol{x}_2 \end{aligned} \tag{4.2}$$

Assuming, as in the previous chapters, that the processes $\boldsymbol{x}_i$ are Gaussian, $\boldsymbol{r}$ has mean $\boldsymbol{\mu}_r$ equal to the difference of the means of the two processes, and $\boldsymbol{R}$ their sum $\boldsymbol{\mu}_R$. Both variables have the same variance $\sigma_r^2 = \sigma_1^2 + \sigma_2^2$. With this, the (appropriately normalized) squared distance $r^2(t)$ between the individuals becomes, in 2D, a noncentral chi-square variable whose distribution has two degrees of freedom

$$u(t) \equiv \frac{r^2(t)}{\sigma_r^2(t)} \sim \chi_2^{2\prime}(\Lambda), \tag{4.3}$$

where $\Lambda \equiv (\boldsymbol{\mu}_1(t) - \boldsymbol{\mu}_2(t))^2 / \sigma_r^2(t)$

We may again define the encounter event as the event of two individuals coming into each other's interaction ranges, i.e., $r^2(t)$ crossing q^2 from above. A problem that has been already analyzed in this context is that of "persistent" interactions given by the stationary rate of encounters as opposed to the initial-condition dependent counting of the first interaction [7].

The difficulty one immediately runs into when looking for first-encounter events between two completely distinct two-dimensional processes is how distance, the proxy for encounters, severely underdetermines, in the general case, the joint probability distribution of $\boldsymbol{r}$ and $\boldsymbol{R}$. Therefore, instead of looking at the

problem in terms of relative distances, we can more directly pose it in terms of a four-dimensional description of the process. That is, we consider the motion given by $\boldsymbol{X}(t) \equiv (\boldsymbol{x}_1(t), \boldsymbol{x}_2(t))$. In this description, we can immediately see that an encounter at a distance q can be described in terms of $\boldsymbol{X}(t)$ hitting the boundary of the region Δ_q defined as

$$\Delta_q \equiv \left\{ (\boldsymbol{x}_1, \boldsymbol{x}_2) \in \mathbb{R}^4 | (\boldsymbol{x}_1 - \boldsymbol{x}_2)^2 \leq q^2 \right\}. \tag{4.4}$$

As such, for the two individual processes $\boldsymbol{x}_i(t)$, $i = 1, 2$ we may write the dynamics in terms of Fokker-Planck equations with operators $L_i(\boldsymbol{x}_i)$. Adding to the state space an absorbing state, as per last chapter, we can, for a given absorption rate function $\omega(\boldsymbol{X})$ supported on Δ_q, write a total "leaky" Fokker-Planck equation

$$\frac{\partial P(\boldsymbol{x}_1, \boldsymbol{x}_2, t)}{\partial t} = \left[L_1(\boldsymbol{x}_1) + L_2(\boldsymbol{x}_2) - \omega(\boldsymbol{x}_1, \boldsymbol{x}_2) \right] P(\boldsymbol{x}_1, \boldsymbol{x}_2, t). \tag{4.5}$$

We may also, as briefly mentioned in the previous chapter, consider partially reflecting boundaries at $\partial\Delta_q$, so that the individuals rigidly collide at a distance q. Whatever the case may be, this defines a general form of the process we use for counting the first probabilistic interaction between two processes. Since the equation (4.5) above simply describes one motion in an effective four-dimensional space, all the techniques previously used to define a backwards equation and integrate over space and time can be used. In particular, if one is simply interested in the mean first-encounter time $\langle T \rangle_q$ as a function of the deterministic initial condition $(\boldsymbol{x}_{10}, \boldsymbol{x}_{20})$, we will have an equation

$$\left[L_1^\dagger(\boldsymbol{x}_{1,0}) + L_2^\dagger(\boldsymbol{x}_{2,0}) \right] \langle T \rangle_q(\boldsymbol{x}_{1,0}, \boldsymbol{x}_{2,0}) = -1, \tag{4.6}$$

$$\langle T \rangle_q |_{\partial\Delta_q} = 0. \tag{4.7}$$

It is in general very difficult to analytically solve any such problem. The symmetries of motion, if any, will likely not coincide with the rotational and translational symmetries of the region Δ_q. One may, nonetheless, construct a particularly symmetric case in which this holds true.

4.2 First-encounter between two identical individuals

Consider two identical individuals living within the same home-range. This may represent, for instance, two members of a pack of social animals. We assume they can both be described as independent realizations of the standard isotropic OU process in 2D, that is

$$\mathrm{d}\boldsymbol{x}_i = \frac{\boldsymbol{x}_i}{\tau}\mathrm{d}t + \sqrt{g}\mathrm{d}\boldsymbol{W}_i(t), \qquad i = 1, 2. \tag{4.8}$$

Because the total motion $\boldsymbol{X}(t)$ too is isotropic and centered at the origin, we can simply reexpress it in terms of the relative coordinates in (4.2). Considering the change of coordinates $(\boldsymbol{x}_1, \boldsymbol{x}_2) \mapsto (\boldsymbol{r}, \boldsymbol{R})$, we can, as in the road problem, assert that motion along the coordinate $\boldsymbol{R}$ cannot affect the interaction statistics — it is simply motion parallel to the plane $\Delta_{q=0}$ which does not affect the relative distance of the individuals. Furthermore, there is rotational symmetry about the same plane. As such, the only variable that can affect the interaction statistics is the distance itself $r(t)$.

It is important to note that the symmetries here refer first and foremost to the symmetries of the equations of motion. In four dimensions, if we call the canonical basis of the plane $(\boldsymbol{e}_1, \boldsymbol{e}_2)$, the change of basis from standard to relative coordinates is given by an orthogonal transformation in $\mathbb{R}^4$, namely

$$(\boldsymbol{e}_{1,1}, \boldsymbol{e}_{2,1}, \boldsymbol{e}_{1,2}, \boldsymbol{e}_{2,2}) \mapsto \left(\frac{\boldsymbol{e}_1 \oplus (-\boldsymbol{e}_1)}{\sqrt{2}}, \frac{\boldsymbol{e}_2 \oplus (-\boldsymbol{e}_2)}{\sqrt{2}}, \frac{\boldsymbol{e}_1 \oplus \boldsymbol{e}_1}{\sqrt{2}}, \frac{\boldsymbol{e}_2 \oplus \boldsymbol{e}_2}{\sqrt{2}} \right). \tag{4.9}$$

Isotropy in the laws of motion means that the functional form of the Fokker-Planck equation is preserved under this transformation. In particular, the motion along the $\boldsymbol{r}$ direction is too given by a Fokker-Planck equation

$$\frac{\partial P(\boldsymbol{r}, t)}{\partial t} = \frac{1}{\tau}\boldsymbol{\nabla}_{\boldsymbol{r}} \cdot (P(\boldsymbol{r}, t)\boldsymbol{r}) + \frac{g}{2}\boldsymbol{\nabla}_{\boldsymbol{r}}^2 P(\boldsymbol{r}, t). \tag{4.10}$$

By isotropy in the $\boldsymbol{r}$-plane as well, we can write the backwards Fokker-Planck equation for the process in the r coordinate as

$$\frac{\partial P(r, t|r_0)}{\partial t} = \left[\left(\frac{g}{2r_0} - \frac{r_0}{\tau} \right) \frac{\partial}{\partial r_0} + \frac{g}{2}\frac{\partial^2}{\partial r_0^2} \right] P(r, t|r_0). \tag{4.11}$$

This leads to the equation for the mean first-passage time at a distance q

$$\left[\left(\frac{g}{2r_0}-\frac{r_0}{\tau}\right)\frac{\mathrm{d}}{\mathrm{d}r_0}+\frac{g}{2}\frac{\mathrm{d}^2}{\mathrm{d}r_0^2}\right]\langle T\rangle_q(r_0)=-1, \tag{4.12}$$

$$\langle T\rangle_q(q)=0, \tag{4.13}$$

$$\langle T\rangle_q'(b\to+\infty)=0. \tag{4.14}$$

It is easy to verify that (by existence and uniqueness) the solution of the equation above is the very simple expression

$$\langle T\rangle_q(r_0)=\tau\log\frac{r_0}{q}. \tag{4.15}$$

We can immediately verify this is exactly the same value as the one obtains with no noise $g=0$, which is just an exponential relaxation process. It is an interesting situation whose generality is not clear, where every initial condition of the deterministic portion of the process hits the boundary. Noise is equally likely to push the system away or toward the absorbing domain, so it vanishes on average.

Note that this reveals an asymptotic behavior which is identical to that of the road problem discussed in Chapter 2, lending support to the universality of this asymptotic behavior in two dimensions. This also agrees exactly with simulation results in Figure 4.2.

This should again be compared to the corresponding results of RBM, for which the equation is, for $b>q>0$, the $\tau\to\infty$ limit of (4.16),

$$\left[\frac{g}{2r_0}\frac{\mathrm{d}}{\mathrm{d}r_0}+\frac{g}{2}\frac{\mathrm{d}^2}{\mathrm{d}r_0^2}\right]\langle T^{\mathrm{RBM}}\rangle_q(r_0)=-1, \tag{4.16}$$

$$\langle T^{\mathrm{RBM}}\rangle_q(q)=0, \tag{4.17}$$

$$\langle T^{\mathrm{RBM}}\rangle_q'(b)=0. \tag{4.18}$$

We can immediately verify that the solution of the homogeneous solution $\langle T^{\mathrm{RBM}}\rangle_q^{(\mathrm{HOM})}$ in terms of two integration constants c_0 and c_1 is

$$\langle T^{\mathrm{RBM}}\rangle_q^{(\mathrm{HOM})}(r_0)=c_1\log(r_0/c_0). \tag{4.19}$$

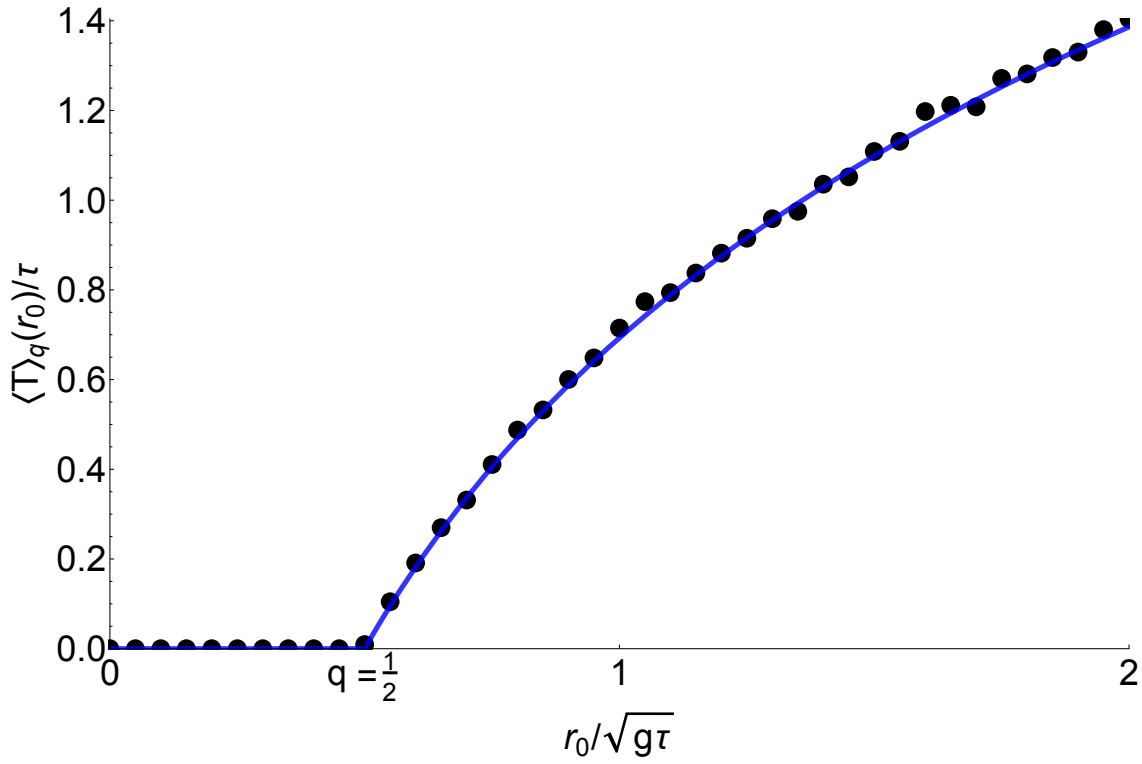

Figure 4.1: First crossing time as a function of the initial separation of two identical OU processes. The points in black are results from numerical simulations, while the blue line is the "exact" result from 4.15.

By starting from a power law *ansatz* $\langle T^{\mathrm{RBM}} \rangle_q^{(0)}(r_0) = \alpha r_0^\beta$ for the particular inhomogeneous solution, we find the diffusive time-scale

$$\langle T^{\mathrm{RBM}} \rangle_q^{(0)}(r_0) = -\frac{1}{2g} r_0^2. \tag{4.20}$$

In the end, we can verify that the full solution is

$$\langle T^{\mathrm{RBM}} \rangle_q(r_0) = \frac{b^2}{g} \log \frac{r_0}{q} + \frac{q^2}{2g} - \frac{r_0^2}{2g}. \tag{4.21}$$

4.3 Discussion and next steps

In this chapter, we have shown how to integrate situations with mutually-interacting individuals into the framework of Chapter 2. This has to be done with care, as the real interactions we are trying to model are often very complex, in such as way that the assumptions made in developing the theory have to be checked.

Even for the simple situations investigated, much work remains to be done.

While it is particularly simple to treat analytically, the situation with two identical individuals does not accurately represent many ecological interactions of interest. Territorial animals of the same species, for example, may have home-ranges of comparable sizes but offset from one another. Predators tend to have much larger home-ranges than their prey, which end up living in a small sub-region of the predator's location. These situations likely cannot be solved analytically, but careful consideration of the scales involved may allow for approximations to be employed.

As compared to the rigid domains of Chapter 3, what probabilistic interactions entail in the case of animals with perceptual ranges will almost always differ. Once two individuals lie within each-others interaction range, there might be an approximately constant rate of absorption acting upon the total system. Finally, there is a question of representing a larger number of individuals. This is also a nontrivial matter given interactions are generally pairwise. It might be interesting to track the various individuals in order of mutual proximity and investigate the statistics of the pairwise interactions — in [31, 32] this is looked at in a particularly simple case of many predators to one prey in Brownian motion, which allows for the easier treatment of such problems due to its conformal invariance.

Chapter 5

Conclusions and future directions

In the present work we have developed a variety of theoretical tools to pose and investigate movement-mediated interactions in home-ranging animals. We have been able to explicitly give a relatively general and simple differential-equation formulation of these scenarios, as well as show how to connect their parameters to the parameters of simulations. By treating multi-individual processes as effective single-individual motions in high dimensions, even interactions between different individuals become a particular case of the framework. Though there are many limitations, the ideas proposed are sufficiently general to allow them to cover such disparate situations as human-wildlife conflict through modified habitats and ecological interactions between individuals.

Nevertheless, there are directions in which this framework itself could be expanded. In particular, one may ask how to connect the absorption rates $\omega(\boldsymbol{x})$ to probabilities $P_a(\boldsymbol{x})$ in the general case, where boundary layer analysis is inadequate as, for example, the absorbing domain may have non-zero volume. This is particularly important in the case of multiple individuals, where besides imposing perfect absorption or a somewhat unrealistic partial reflection, the only way to make sense of the region $0 < r < q$ is to insert a finite, non-zero value of ω in the domain.

There are, furthermore, many questions to be investigated in how to utilize these models to investigate larger scale phenomena. For example, given some number of home-ranges in a region, optimizing the construction of a feature to minimize interactions with animals can be quite clearly posed mathematically in terms of movement here. It would also be interesting to more explicitly connect these results to population dynamics models and results in encounter rates, understanding the precise assumptions that allow these models to work.

In summary, we leave here a work that is open to be extended in various directions. Though we have taken small steps, we certainly believe they can contribute to the increasingly large theoretical effort in describing ecological phenomena quantitatively. We hope that, by developing tools that allows questions

to be posed mechanistically, new insights into animal movement ecology may be gained.

Bibliography

[1] Sabina Leonelli. The challenges of big data biology. *eLife*, 8:e47381, April 2019. Publisher: eLife Sciences Publications, Ltd.

[2] Ran Nathan, Christopher T. Monk, Robert Arlinghaus, Timo Adam, Josep Alós, Michael Assaf, Henrik Baktoft, Christine E. Beardsworth, Michael G. Bertram, Allert I. Bijleveld, Tomas Brodin, Jill L. Brooks, Andrea Campos-Candela, Steven J. Cooke, Karl Ø Gjelland, Pratik R. Gupte, Roi Harel, Gustav Hellström, Florian Jeltsch, Shaun S. Killen, Thomas Klefoth, Roland Langrock, Robert J. Lennox, Emmanuel Lourie, Joah R. Madden, Yotam Orchan, Ine S. Pauwels, Milan Říha, Manuel Roeleke, Ulrike E. Schlägel, David Shohami, Johannes Signer, Sivan Toledo, Ohad Vilk, Samuel Westrelin, Mark A. Whiteside, and Ivan Jarić. Big-data approaches lead to an increased understanding of the ecology of animal movement. *Science (New York, N.Y.)*, 375(6582):eabg1780, February 2022.

[3] Mitra Baratchi, Nirvana Meratnia, Paul J. M. Havinga, Andrew K. Skidmore, and Bert A. G. Toxopeus. Sensing solutions for collecting spatio-temporal data for wildlife monitoring applications: a review. *Sensors (Basel, Switzerland)*, 13(5):6054–6088, May 2013.

[4] Jarrod C. Hodgson, Shane M. Baylis, Rowan Mott, Ashley Herrod, and Rohan H. Clarke. Precision wildlife monitoring using unmanned aerial vehicles. *Scientific Reports*, 6:22574, March 2016.

[5] Ran Nathan, Wayne M. Getz, Eloy Revilla, Marcel Holyoak, Ronen Kadmon, David Saltz, and Peter E. Smouse. A movement ecology paradigm for unifying organismal movement research. *Proceedings of the National Academy of Sciences*, 105(49):19052–19059, December 2008. Publisher: Proceedings of the National Academy of Sciences.

[6] P. G. Blackwell. Random diffusion models for animal movement. *Ecological Modelling*, 100(1):87–102, December 1997.

[7] Ricardo Martinez-Garcia, Christen H. Fleming, Ralf Seppelt, William F. Fagan,

and Justin M. Calabrese. How range residency and long-range perception change encounter rates. *Journal of Theoretical Biology*, 498:110267, August 2020.

[8] N. G. Van Kampen. *Stochastic Processes in Physics and Chemistry*. Elsevier, August 2011.

[9] Vicenç Méndez, Daniel Campos, and Frederic Bartumeus. *Stochastic Foundations in Movement Ecology: Anomalous Diffusion, Front Propagation and Random Searches*. Springer, New York, 2014ª edição edition, 2013.

[10] G. E. Uhlenbeck and L. S. Ornstein. On the Theory of the Brownian Motion. *Physical Review*, 36(5):823–841, September 1930. Publisher: American Physical Society.

[11] Crispin Gardiner. *Stochastic Methods: A Handbook for the Natural and Social Sciences: 13*. Springer, Berlin, 4th 2009 ed. edição edition, January 2009.

[12] Weinan E, Tiejun Li, and Eric Vanden-eijnden. *Applied Stochastic Analysis*. American Mathematical Society, Providence, Rhode Island, May 2019.

[13] James E. Dunn and Phillip S. Gipson. Analysis of Radio Telemetry Data in Studies of Home Range. *Biometrics*, 33(1):85–101, 1977. Publisher: [Wiley, International Biometric Society].

[14] Michael J. Noonan, Ricardo Martinez-Garcia, Grace H. Davis, Margaret C. Crofoot, Roland Kays, Ben T. Hirsch, Damien Caillaud, Eric Payne, Andrew Sih, David L. Sinn, Orr Spiegel, William F. Fagan, Christen H. Fleming, and Justin M. Calabrese. Estimating encounter location distributions from animal tracking data. *Methods in Ecology and Evolution*, 12(7):1158–1173, 2021. _eprint: https://onlinelibrary.wiley.com/doi/pdf/10.1111/2041-210X.13597.

[15] Oscar Venter, Eric W. Sanderson, Ainhoa Magrach, James R. Allan, Jutta Beher, Kendall R. Jones, Hugh P. Possingham, William F. Laurance, Peter Wood, Balázs M. Fekete, Marc A. Levy, and James E. M. Watson. Sixteen years of change in the global terrestrial human footprint and implications for biodiversity conservation. *Nature Communications*, 7(1):12558, August 2016. Number: 1 Publisher: Nature Publishing Group.

[16] Erin K. Buchholtz, Amanda Stronza, Anna Songhurst, Graham McCulloch, and Lee A. Fitzgerald. Using landscape connectivity to predict human-wildlife conflict. *Biological Conservation*, 248:108677, August 2020.

[17] Scott R. Loarie, Rudi J. Van Aarde, and Stuart L. Pimm. Fences and artificial water affect African savannah elephant movement patterns. *Biological Conservation*, 142(12):3086–3098, December 2009.

[18] Natalia Rebolo-Ifrán, Pablo Plaza, Juan Manuel Pérez-García, Víctor Gamarra-Toledo, Francisco Santander, and Sergio A. Lambertucci. Power lines and birds: An overlooked threat in South America. *Perspectives in Ecology and Conservation*, December 2022.

[19] M. J. Noonan, F. Ascensão, D. R. Yogui, and A. L. J. Desbiez. Roads as ecological traps for giant anteaters. *Animal Conservation*, 25(2):182–194, 2022. _eprint: https://onlinelibrary.wiley.com/doi/pdf/10.1111/acv.12728.

[20] David J. Griffiths. *Introduction to Electrodynamics*. Cambridge University Press, Cambridge, United Kingdom ; New York, NY, 4th revised ed. edição edition, June 2017.

[21] Arnold J. F. Siegert. On the First Passage Time Probability Problem. *Physical Review*, 81(4):617–623, February 1951. Publisher: American Physical Society.

[22] Luigi M. Ricciardi and Shunsuke Sato. First-Passage-Time Density and Moments of the Ornstein-Uhlenbeck Process. *Journal of Applied Probability*, 25(1):43–57, 1988. Publisher: Applied Probability Trust.

[23] L. Alili, P. Patie, and J. L. Pedersen. Representations of the First Hitting Time Density of an Ornstein-Uhlenbeck Process. *Stochastic Models*, 21(4):967–980, October 2005. Publisher: Taylor & Francis _eprint: https://doi.org/10.1080/15326340500294702.

[24] David Hartich and Aljaž Godec. Interlacing relaxation and first-passage phenomena in reversible discrete and continuous space Markovian dynamics. *Journal of Statistical Mechanics: Theory and Experiment*, 2019(2):024002, February 2019. Publisher: IOP Publishing and SISSA.

[25] A. Singer and Z. Schuss. Brownian simulations and unidirectional flux in diffusion. *Physical Review E*, 71(2):026115, February 2005. Publisher: American Physical Society.

[26] A. Singer, Z. Schuss, A. Osipov, and D. Holcman. Partially Reflected Diffusion. *SIAM Journal on Applied Mathematics*, 68(3):844–868, 2007. Publisher: Society for Industrial and Applied Mathematics.

[27] Radek Erban and S. Jonathan Chapman. Reactive boundary conditions for stochastic simulations of reaction–diffusion processes. *Physical Biology*, 4(1):16–28, February 2007. Publisher: IOP Publishing.

[28] Raúl Toral and Pere Colet. *Stochastic Numerical Methods: An Introduction for Students and Scientists*. Wiley-VCH, Weinheim, 1st edition edition, August 2014.

[29] A. J. Bengsen, D. Algar, G. Ballard, T. Buckmaster, S. Comer, P. J. S. Fleming, J. A. Friend, M. Johnston, H. McGregor, K. Moseby, and F. Zewe. Feral cat home-range size varies predictably with landscape productivity and population density. *Journal of Zoology*, 298(2):112–120, 2016. _eprint: https://onlinelibrary.wiley.com/doi/pdf/10.1111/jzo.12290.

[30] Melanie Dickie, Robert Serrouya, Tal Avgar, Philip McLoughlin, R. Scott McNay, Craig DeMars, Stan Boutin, and Adam T. Ford. Resource exploitation efficiency collapses the home range of an apex predator. *Ecology*, 103(5):e3642, 2022. _eprint: https://onlinelibrary.wiley.com/doi/pdf/10.1002/ecy.3642.

[31] George Herbert Weiss. *Aspects and Applications of the Random Walk*. North-Holland, 1994. Google-Books-ID: QRnvAAAAMAAJ.

[32] S. Redner. A First Look at First-Passage Processes, February 2022. arXiv:2201.10048 [cond-mat].